Annu. Rev. Astron. Astrophys. 2000. 38:143–90

THE EVOLUTION OF ROTATING STARS

André Maeder and Georges Meynet
Geneva Observatory, CH–1290 Sauverny, Switzerland;
e-mail: andre.maeder@obs.unige.ch, georges.meynet@obs.unige.ch

Key Words stellar rotation, stellar evolution, mass loss, mixing, chemical abundances

■ **Abstract** In this article we first review the main physical effects to be considered in the building of evolutionary models of rotating stars on the Upper Main-Sequence (MS). The internal rotation law evolves as a result of contraction and expansion, meridional circulation, diffusion processes, and mass loss. In turn, differential rotation and mixing exert a feedback on circulation and diffusion, so that a consistent treatment is necessary.

We review recent results on the evolution of internal rotation and the surface rotational velocities for stars on the Upper MS, for red giants, supergiants, and W-R stars. A fast rotation enhances the mass loss by stellar winds and, conversely, high mass loss removes a lot of angular momentum. The problem of the breakup or Ω-limit is critically examined in connection with the origin of Be and LBV stars. The effects of rotation on the tracks in the HR diagram, the lifetimes, the isochrones, the blue-to-red supergiant ratios, the formation of Wolf-Rayet stars, and the chemical abundances in massive stars as well as in red giants and AGB stars are reviewed in relation to recent observations for stars in the Galaxy and Magellanic Clouds. The effects of rotation on the final stages and on the chemical yields are examined, along with the constraints placed by the periods of pulsars. On the whole, this review points out that stellar evolution is not only a function of mass M and metallicity Z, but of angular velocity Ω as well.

1. INTRODUCTION

Stellar rotation is an example of an astronomical domain that has been studied for several centuries and in which the developments are rather slow. A short historical review since the discovery of the solar rotation by Galileo Galilei is given by Tassoul (1978). Few of the early works apply to real stars, because in general gaseous configurations were not considered, and no account was given to radiative energy transport. The equations of rotating stars in radiative equilibrium were first considered by Milne (1923), von Zeipel (1924) and Eddington (1925); see also Tassoul (1990) for a more recent history. From the early days of stellar evolution, the studies of rotation and evolution have been closely associated. Soon after the first models showing that Main-Sequence (MS) stars move farther into the giant

and supergiant region (Sandage & Schwarzschild 1952), rotation was used as a major test for the evolution. Oke & Greenstein (1954) and Sandage (1955) found that the observed rotational velocities were consistent with the proposed evolutionary sequence.

Stellar evolution, like other fields of science, proceeds using as a guideline the principle of Occam's razor, which says that the explanation relying on the smallest number of hypotheses is usually the one to be preferred. Thus, as a result of the many well-known successes of the theory of stellar evolution, rotation was and is still generally considered only a second order effect. Over recent years, however, a number of serious discrepancies between current models and observations have been noticed. They particularly concern the helium and nitrogen abundances in massive O- and B-type stars and in giants and supergiants, as well as the distribution of stars in the HR diagram at various metallicities. The observations show that the role of rotation has been largely overlooked. All the model outputs (tracks in the HR diagram, lifetimes, actual masses, surface abundances, nucleosynthetic yields, supernova precursors, etc) are greatly influenced by rotation; thus, it turns out that stellar evolution is basically a function of mass M, metallicity Z, and angular velocity Ω.

A number of reviews exist concerning stellar rotation—for example, Strittmatter (1969), Fricke & Kippenhahn (1972), Tassoul (1978, 1990), Zahn (1983, 1994) and Pinsonneault (1997). Here, we focus on rotation in Upper MS stars, where the effects are likely the largest ones. The consequences for blue, yellow, and red supergiants and Wolf-Rayet (W-R) stars, as well as for red giants and Asymptotic Giant Branch (AGB) stars, are also examined. The rotation of low-mass stars, where spin-down resulting from magnetic coupling between the wind and the central body is important, has been treated in a recent review (Pinsonneault 1997); rotation and magnetic activity were also reviewed by Hartmann & Noyes (1987). The role of rotation in pre-Main Sequence evolution with accretion disks has been discussed by Bodenheimer (1995).

2. BASIC PHYSICAL EFFECTS OF ROTATION

2.1 Hydrostatic Effects

In a rotating star, the centrifugal forces reduce the effective gravity according to the latitude and also introduce deviations from sphericity. The four equations of stellar structure need to be modified. The idea of the original method devised by Kippenhahn & Thomas (1970) and applied in most subsequent works (Endal & Sofia 1976; Pinsonneault et al 1989, 1990, 1991; Fliegner & Langer 1995; Heger et al 2000) is to replace the usual spherical eulerian or lagrangian coordinates with new coordinates characterizing the equipotentials. This method applies when the effective gravity can be derived from a potential, i.e. when the problem is conservative, which occurs for solid body rotation or for constant rotation on

cylinders centered on the axis of rotation. If so, the structural variables P, T, ρ, ... are constant on an equipotential $\Psi = \Phi + \frac{1}{2}\Omega^2 r^2 \sin^2 \vartheta$, where Φ is the gravitational potential, ϑ is the colatitude, and Ω is the angular velocity. Thus the problem can be kept one-dimensional, which is a major advantage. However, the internal rotation generally evolves toward rotation laws that are non-conservative; in this case the above method is not physically consistent. Unfortunately, it has been and is still used by most authors.

A particularly interesting case of differential rotation is that with Ω constant on isobars (Zahn 1992). This case is called "shellular rotation," and it is often approximated by $\Omega = \Omega(r)$, which is valid at low rotation. It is supported by the study of turbulence in the Sun and stars (Spiegel & Zahn 1992, Zahn 1992). Such a law results from the fact that the turbulence is very anisotropic, with a much stronger, geostrophic-like transport in the horizontal direction than in the vertical one, where stabilization is favored by the stable temperature gradient. The horizontal turbulence enforces an essentially constant rotation rate on isobars, thus producing the preceding rotation law. The star models are essentially one-dimensional, which enormously simplifies the computations. Shellular rotation is likely to occur in fast as well as in slow rotators.

The equations of stellar structure can be written consistently for a differentially rotating star, if the rotation law is shellular. Then, the isobaric surfaces satisfy the same equation $\Psi = const.$ as the equipotentials of the conservative case (Meynet & Maeder 1997), and thus the equations of stellar structure can be written as a function of the coordinate of an isobar, either in the lagrangian or eulerian form. Let us emphasize that in general the hydrostatic effects of rotation have only very small effects of the order of a few percent on the internal evolution (Faulkner et al 1968, Kippenhahn & Thomas 1970). Recent two-dimensional models including the hydrostatic effects of rotation confirm the smallness of these effects (Shindo et al 1997).

The above potential Ψ describes the shape of the star in the conservative case for the so-called Roche model, where the distortions of the gravitational potential are neglected. However, the stellar surface deviates from a surface given by $\Psi = const.$ in the case of non-conservative rotation law (Kippenhahn 1977).

2.2 The von Zeipel Theorem

The von Zeipel (1924) theorem is essential for predicting the distribution of temperature at the surface of a rotating star. It applies to the conservative case and states that the local radiative flux $\vec{F}$ is proportional to the local effective gravity $\vec{g_{\rm eff}}$, which is the sum of the gravity and centrifugal force, if the star is not close to the Eddington limit,

$$\vec{F} = -\frac{L(P)}{4\pi G M_\star(P)}\,\vec{g_{\rm eff}}, \qquad (1)$$

with $M_\star(P) = M(1 - \frac{\Omega^2}{2\pi G\bar{\rho}})$; $L(P)$ is the luminosity on an isobar, and $\bar{\rho}$ is the mean internal density. Thus, the local effective temperature on the surface of a rotating star varies like $T_{\rm eff}(\vartheta) \sim g_{\rm eff}(\vartheta)^{\frac{1}{4}}$. This shows that the spectrum of a rotating star is in fact a composite spectrum made up of local atmospheres of different gravity and $T_{\rm eff}$. If it is meaningful to define an average, a reasonable choice is to take $T_{\rm eff}^4 = L/(\sigma S(\Omega))$, where σ is Stefan's constant and $S(\Omega)$ is the total actual stellar surface. In the case of non-conservative rotation law, the corrections to the von Zeipel theorem depend on the opacity law and on the degree of differential rotation, but the corrections are likely to be small, i.e. $\leq$1% in current cases of shellular rotation (Kippenhahn 1977, Maeder 1999a). There are some discussions (Langer 1999; Langer et al 1999a) as to whether von Zeipel must really be used; we would like to emphasize that this is a mere and inescapable consequence of Newton's law and basic thermodynamics (see Section 5.3).

2.3 Transport of Angular Momentum and Chemical Elements

Inside a rotating star the angular momentum is transported by convection, turbulent diffusion, and meridional circulation. The equation of transport was derived by Jeans (1928), Tassoul (1978), Chaboyer & Zahn (1992), and Zahn (1992). For shellular rotation, the equation of transport of angular momentum in the vertical direction is (in lagrangian coordinates)

$$\rho \frac{d}{dt}(r^2\Omega)_{M_r} = \frac{1}{5r^2}\frac{\partial}{\partial r}(\rho r^4 \Omega U(r)) + \frac{1}{r^2}\frac{\partial}{\partial r}\left(\rho D r^4 \frac{\partial \Omega}{\partial r}\right). \qquad (2)$$

$\Omega(r)$ is the mean angular velocity at level r, $U(r)$ is the vertical component of the meridional circulation velocity, and D is the diffusion coefficient resulting from the sum of the various turbulent diffusion processes (see Section 2.5). The factor $\frac{1}{5}$ comes from the integration in latitude. If both $U(r)$ and D are zero, we just have the local conservation of the angular momentum $r^2\Omega = const.$ for a fluid element in case of contraction or expansion. The solution of Equation 2 gives the *non-stationary solution* of the problem. The rotation law is not arbitrarily chosen, but is allowed to evolve with time as a result of transport by meridional circulation, diffusion processes, and contraction or expansion. In turn, the differential rotation built up by these processes generates some turbulence and meridional circulation, which are themselves functions of the rotation law. This coupling provides feedback, and the self-consistent solution for the evolution of $\Omega(r)$ must be found (Zahn 1992).

Some characteristic times can be associated to both the processes of meridional circulation and diffusion:

$$t_{\rm circ} \simeq \frac{R}{U}, \qquad t_{\rm diff} \simeq \frac{R^2}{D}. \qquad (3)$$

These timescales are essential quantities, because the comparison with the nuclear timescales will show the relative importance of the transport processes in the considered nuclear phases. Equation 2 also admits a *stationary solution* when one of the above characteristic times is short with respect to the nuclear evolution time, a situation that only occurs at the beginning of the MS:

$$U(r) = -\frac{5D}{\Omega}\frac{\partial \Omega}{\partial r}. \tag{4}$$

This equation (Randers 1941, Zahn 1992) expresses that the (inward) flux of angular momentum transported by meridional circulation is equal to the (outward) diffusive flux of angular momentum. As a matter of fact, this solution is equivalent to considering local conservation of angular momentum (Urpin et al 1996).

Instead of Equation 2, the transport of angular momentum by circulation is often treated as a diffusion process (Endal & Sofia 1978; Pinsonneault et al 1989, 1990; Langer 1991a; Fliegner & Langer 1995; Chaboyer et al 1995a,b; Heger et al 2000). We see from Equation 2 that the term with U (advection) is functionally not the same as the term with D (diffusion). Physically, advection and diffusion are quite different. Diffusion brings a quantity from where there is a lot of this quantity to other places where there is little. This is not necessarily the case for advection; for example, the circulation of money in the world is not a diffusive process, but an advective one. Let us make it clear that circulation with a positive value of $U(r)$, i.e. rising along the polar axis and descending at the equator, is in fact making an *inward* transport of angular momentum. If this process were treated as a diffusive function of $\frac{\partial \Omega}{\partial r}$, even the sign of the effect may be wrong.

A differential equation like Equation 2 is subject to boundary conditions at the edge of the core and at the stellar surface. At both places, this condition is usually $\frac{\partial \Omega}{\partial r} = 0$, with in addition the assumptions of solid body rotation for the convective core and $U = 0$ at the surface (Talon et al 1997, Denissenkov et al 1999). If there is magnetic coupling at the surface (Hartmann & Noyes 1987; Pinsonneault et al 1989, 1990; Pinsonneault 1997) or mass loss by stellar winds, the surface condition must be modified accordingly (Maeder 1999a). Various asymptotic regimes for the angular momentum transport can be considered (Zahn 1992) depending on the presence of a wind with or without magnetic coupling.

2.3.1 Transport of Chemical Elements The transport of chemical elements is also governed by a diffusion–advection equation like Equation 2 (Endal & Sofia 1978; Schatzman et al 1981; Langer 1991a, 1992; Heger et al 2000). However, if the horizontal component of the turbulent diffusion is large, the vertical advection of the elements (and not that of the angular momentum) can be treated as a simple diffusion (Chaboyer & Zahn 1992) with a diffusion coefficient $D_{\rm eff}$,

$$D_{\rm eff} = \frac{|rU(r)|^2}{30D_h}, \tag{5}$$

where D_h is the coefficient of horizontal turbulence, for which an estimate is $D_h = |rU(r)|$ (Zahn 1992). Equation 5 expresses that the vertical advection of chemical elements is severely inhibited by the strong horizontal turbulence characterized by D_h. Thus, the change of the mass fraction X_i of the chemical species i is simply

$$\left(\frac{dX_i}{dt}\right)_{M_r} = \left(\frac{\partial}{\partial M_r}\right)_t \left[(4\pi r^2\rho)^2 D_{\rm mix}\left(\frac{\partial X_i}{\partial M_r}\right)_t\right] + \left(\frac{dX_i}{dt}\right)_{\rm nucl}. \quad (6)$$

The second term on the right accounts for composition changes resulting from nuclear reactions. The coefficient $D_{\rm mix}$ is the sum $D_{\rm mix} = D + D_{\rm eff}$, where D is the term appearing in Equation 2 and $D_{\rm eff}$ accounts for the combined effect of advection and horizontal turbulence. The characteristic time for the mixing of chemical elements is therefore

$$t_{\rm mix} \simeq \frac{R^2}{D_{\rm mix}}. \quad (7)$$

Noticeably, the characteristic time for chemical mixing is not $t_{\rm circ}$ given by Equation 3, as has been generally assumed (Schwarzschild 1958). This makes the mixing of the chemical elements much slower, since $D_{\rm eff}$ is very much reduced. In this context, we recall that several authors have reduced by arbitrary factors (up to 30 or 100) the effect of the transport of chemicals in order to better fit the observed surface compositions (Pinsonneault et al 1989, 1991; Chaboyer et al 1995a,b; Heger et al 2000). This is no longer necessary with the more appropriate expressions given above.

2.4 Meridional Circulation

Meridional circulation arises from the local breakdown of radiative equilibrium in a rotating star (Vogt 1925, Eddington 1925). In a uniformly rotating star, the equipotentials are closer to each other along the polar axis than along the equatorial axis. Thus, according to von Zeipel's theorem, the heating on an equipotential is generally higher in the polar direction than in the equatorial direction, which thus drives a large-scale circulation rising at the pole and descending at the equator. This problem has been studied for about 75 years (see reviews by Tassoul 1978 or Zahn 1983). The classical formulation (Sweet 1950; Mestel 1953, 1965; Kippenhahn & Weigert 1990) for rigid rotation predicts a value of the vertical velocity of the Eddington-Sweet circulation

$$U_{ES} = \frac{8}{3}\omega^2 \frac{L}{gM}\frac{\gamma-1}{\gamma}\frac{1}{\nabla_{\rm ad}-\nabla}\left(1-\frac{\Omega^2}{2\pi G\rho}\right), \quad (8)$$

with $\omega^2 = \frac{\Omega^2 r^3}{GM_r}$ the local ratio of centrifugal force to gravity and γ the ratio of the specific heats C_P/C_V. The term $\frac{\Omega^2}{2\pi G\rho}$, often called the Gratton-Öpik term (Tassoul

1990), predicts that U_{ES} becomes negative at the stellar surface because of the presence of the term $1/\rho$. This means an inverse circulation, i.e. descending at the pole and rising at the equator. The dependence in $\frac{1}{\rho}$ also makes $U(r)$ diverge at the surface. This has led to some controversies on what is limiting $U(r)$ (Tassoul & Tassoul 1982, 1995; Zahn 1983; Tassoul 1990). The timescale for circulation mixing defined in Equation 3 becomes, with the above Eddington-Sweet velocity,

$$t_{\rm ES} \simeq t_{\rm KH} \frac{g}{\Omega^2 R}, \tag{9}$$

where g is the surface gravity and R is the stellar radius. Even for modest rotation velocities, $t_{\rm ES}$ is much shorter than the MS lifetime (Schwarzschild 1958; see also Denissenkov et al 1999), so that most stars should be mixed, if this timescale were applicable. However, the presence of μ-gradients was not taken into account in the above expressions. When this is done, rotation is found to allow circulation above only a certain rotation limit that depends on the value of the μ-gradient (Mestel 1965, Kippenhahn 1974, Kippenhahn & Weigert 1990). The balance of rotation and μ-gradients has been considered in Vauclair (1999).

The velocity of the meridional circulation in the case of shellular rotation was derived by Zahn (1992), who considered the effects of the latitude-dependent μ-distribution (Mestel 1953, 1965). Even more important are the effects of the vertical μ-gradient ∇_μ and of the horizontal turbulence (Maeder & Zahn 1998). Contrary to the conclusions of the previous works, the μ-gradients were shown not to introduce a velocity threshold for the existence of the circulation, but to progressively reduce the circulation when ∇_μ increases. We then have

$$U(r) = \frac{P}{\rho g C_P T \left[\nabla_{\rm ad} - \nabla + (\varphi/\delta)\nabla_\mu\right]} \left\{ \frac{L}{M_\star}(E_\Omega + E_\mu) \right\}, \tag{10}$$

where P is the pressure, C_P is the specific heat, and E_Ω and E_μ are terms depending on the Ω- and μ-distributions respectively, up to the third-order derivatives. Because the derivative of $U(r)$ appears in Equation 2, we see that the consistent solution to the problem is of fourth order (Zahn 1992). This makes the numerical solution difficult (Talon et al 1997, Denissenkov et al 1999, Meynet & Maeder 2000). Whereas the classical solution predicts an infinite velocity at the interface between a radiative and a semiconvective zone with an inverse circulation in the semiconvective zone, Equation 10 gives a continuity of the solution with no change of sign. In evolutionary models, the term ∇_μ in Equation 10 may be one or two orders of magnitude larger than $\nabla_{\rm ad} - \nabla$ in some layers, so that $U(r)$ may be reduced by the same ratio. This considerably increases the characteristic time $t_{\rm circ}$ with respect to the classical estimate $t_{\rm ES}$.

2.5 Instabilities and Transport

The subject of the instabilities in moving plasmas is a field in itself. Here we limit ourselves to a short description of the main instabilities currently considered

influential in the evolution of Upper MS stars (Endal & Sofia 1978; Zahn 1983, 1992; Pinsonneault et al 1989; Heger et al 2000).

2.5.1 Convective and Solberg-Høiland Instability In a rotating star, the Ledoux or Schwarzschild criteria for convective instability should be replaced by the Solberg–Høiland criterion (Kippenhahn & Weigert 1990). This criterion accounts for the difference of the centrifugal force for an adiabatically displaced fluid element; the condition for dynamical stability is

$$N^2 + \frac{1}{s^3}\frac{d(s^2\Omega)^2}{ds} \geq 0. \tag{11}$$

The Brunt-Väisälä frequency N^2 is given by $N^2 = \frac{g\delta}{H_p}(\nabla_{\rm ad} - \nabla + \frac{\varphi}{\delta}\nabla_\mu)$, where the various symbols have their usual meaning (Kippenhahn & Weigert 1990), and the term s is the distance to the rotation axis. For no rotation, the Ledoux criterion is recovered. If the thermal effects are ignored, we just recover Rayleigh's criterion for stability, which says that the specific angular momentum $s^2\Omega$ must increase with the distance to the rotation axis. For displacements parallel to the rotation axis, convective instability occurs when $N^2 < 0$. For displacements perpendicular to the rotation axis, the stability is in general reinforced. Thus, criterion (Equation 11) is sensitive to the type of axisymmetric displacements considered (cf. Ledoux 1958). In the absence of rotation, a zone located beween the places where $\nabla = \nabla_{\rm ad} + \nabla_\mu$ and $\nabla = \nabla_{\rm ad}$ is called semiconvective. There, non-adiabatic effects can drive growing oscillatory instabilities (Kato 1966, Kippenhahn & Weigert 1990). An appropriate diffusion coefficient describing the transport in such zones was derived by Langer et al (1983). However, there is no diffusion coefficient yet available for semiconvective mixing in the presence of rotation.

The assumption of solid body rotation is generally made in convective regions, owing to the strong turbulent coupling. However, the collisions or scattering of convective blobs influence the rotation law in convective regions (Kumar et al 1995): Solid body rotation only occurs for an isotropic scattering. For some forms of anisotropic scattering, an outward rising rotation profile such as that observed in the Sun can be produced. Two-dimensional models of rotating stars (Deupree 1995, 1998) also show that the angular velocity in convective cores is not uniform, but it decreases with distance from the center and is about constant on cylinders. A considerable overshoot is obtained by Deupree (1998) and amounts to about 0.35 H_P, where H_P is the local pressure scale height. Similar conclusions were obtained by Toomre (1994), who also found penetrative convection at the edge of the convective core of rotating A-type stars. The very large Reynolds number characterizing stellar turbulence prevents direct numerical simulations of the Navier-Stokes equation, so that some new specific methods have been proposed to study convective turbulence (Canuto 1994, Canuto et al 1996, Canuto & Dubovikov 1997) and its interplay with differential rotation (Canuto et al 1994, Canuto 1998); these last results have not yet been applied to evolutionary models in rotation.

2.5.2 Shear Instabilities: Dynamical and Secular In a radiative zone, shear caused by differential rotation is likely to be a very efficient mixing process. Indeed, shear instability grows on a dynamical timescale that is of the order of the rotation period (Zahn 1992, 1994). Stability is maintained when the Richardson number *Ri* is larger than a critical value $Ri_{\rm cr}$

$$Ri = \frac{N^2}{\left(\frac{dV}{dz}\right)^2} > Ri_{\rm cr} = \frac{1}{4}, \tag{12}$$

where V is the horizontal velocity and z is the vertical coordinate. Equation 12 means that the restoring force of the density gradient is larger than the excess energy $\frac{1}{4}\left(\frac{dV}{dz}\right)^2$ present in the differentially rotating layers (Chandrasekhar 1961). In Equation 12, heat exchanges are ignored and the criterion refers to the dynamical shear instability (Endal & Sofia 1978, Kippenhahn & Weigert 1990).

When thermal dissipation is significant, the restoring force of buoyancy is reduced and the instability occurs more easily (Endal & Sofia 1978); the timescale is longer, however, because it is the thermal timescale. This case is sometimes referred to as secular shear instability. For small thermal effects ($Pe \ll 1$), a factor equal to *Pe* appears as multiplying N^2 in Equation 12 (Zahn 1974). The number *Pe* is the ratio of the thermal cooling time to the dynamical time, i.e. $Pe = \frac{v\ell}{K}$, where v and ℓ are the characteristic velocity and length scales, and $K = (4acT^3)/(3C_P\kappa\rho^2)$ is the thermal diffusivity. *Pe* varies typically from 10^9 in deep interiors to 10^{-2} in outer layers (Cox & Giuli 1968). For general values of *Pe*, a more general expression of the Richardson's criterion can be found (Maeder 1995, Maeder & Meynet 1996); it is consistent with the case of low *Pe* treated by Zahn (1974). The problem of the Richardson criterion has also been considered by Canuto (1998), who suggests that for $Pe > 1$, i.e. negligible radiative losses $Ri_{\rm cr} \sim 1$, and for $Pe < 1$, i.e. important radiative losses $Ri_{\rm cr} \sim Pe^{-1}$. Thus, similar dependences with respect to *Pe* are obtained, but Canuto (1998) finds that turbulence may exist beyond the $\frac{1}{4}$ limit in Equation 12.

Many authors have shown that the μ-gradients appear to inhibit the mixing too much with respect to what is required by the observations (Chaboyer et al 1995a,b; Meynet & Maeder 1997). Changing $Ri_{\rm cr}$ from $\frac{1}{4}$ to 1 does not solve the problem, since the difference is a matter of one or two orders of magnitude. For example, instead of using a gradient ∇_μ, some authors write $f_\mu \nabla_\mu$ with an arbitrary factor $f_\mu = 0.05$ or even smaller (Heger et al 2000; see also Chaboyer et al 1995a,b). Most of the zone external to the convective core, where the μ-gradient inhibits mixing, is in fact semiconvective and is thus subject to thermal instability anyway. This has led to the hypothesis that the excess energy in the shear is degraded by turbulence on the thermal timescale, which changes the entropy gradient and consequently the μ-gradient (Maeder 1997). This gives a diffusion coefficient $D_{\rm shear}$, which tends toward the diffusion coefficient for semiconvection by Langer et al (1983) when shear is negligible and toward the value $D_{\rm shear} = (K/N^2)(\Omega \frac{d \ln \Omega}{d \ln r})^2$ given by Zahn (1992) when semiconvection is negligible. Another proposition was made

by Talon & Zahn (1997), who took into account the homogeneizing effect of the horizontal diffusion on the restoring force produced by the μ-gradient. This also reduces the excessive stabilizing effect of the μ-gradient. Both of the above suggestions lead to an acceptable amount of mixing in view of the observations. We stress that the Reynolds condition $D_{\rm shear} \geq \frac{1}{3}\nu Re_c$ must be satisfied when the medium is turbulent, where Re_c is the critical Reynolds number (Zahn 1992, Denissenkov et al 1999) and ν is the total viscosity (radiative + molecular).

Globally, we may expect the secular instability to work during the MS phase, where the Ω-gradients are small and the lifetimes are long, whereas the dynamical instability could play a role in the advanced stages.

2.5.3 Other Instabilities Baroclinicity, i.e. the non-coincidence of the equipotentials and surface of constant ρ, generates various instabilities in the case of non-conservative rotation laws. Some instabilities are axisymmetric, like the GSF instability (Goldreich & Schubert 1967, Fricke 1968, Korycansky 1991). The GSF instability is created by fluid elements displaced between the directions of constant angular momentum and of the rotational axis. Stability demands a uniform or constant rotation on cylinders, which is incompatible with shellular rotation. The GSF instability thus favors solid-body rotation, on a timescale of the order of that of the meridional circulation (Endal & Sofia 1978). This instability is inhibited by the μ-gradients (Knobloch & Spruit 1983), nevertheless Heger et al (2000) find that it plays a role near the end of the helium-burning phase. Another axisymmetric instability is the ABCD instability (Knobloch & Spruit 1983). Fluid elements displaced between the surfaces of constant P and T create the ABCD instability, a kind of horizontal convection. The ABCD instability is oscillatory, and its efficiency is difficult to estimate for now. Non-axisymmetric instabilities, such as salt-fingers, may also occur (Spruit & Knobloch 1984). They are not efficient when rotation is low; however, in the case of fast rotation they may occur everywhere in rotating stars, so that one-dimensional models are likely to be an unsatisfactory idealization in this case.

The study of the transport of angular momentum by gravity waves has been stimulated by the finding of an almost solid body rotation for most of the radiative interior of the Sun (Schatzman 1993, Montalban 1994, Kumar & Quataert 1997, Zahn et al 1997, Talon & Zahn 1998). Gravity waves are supposed to transport angular momentum from the external convective layers to the radiative interior. However, Ringot (1998) has recently shown that quasi-solid rotation of the radiative zone of the Sun cannot be a direct consequence of the action of gravity waves. Thus, even for the Sun the importance of gravity waves remains uncertain.

In Upper MS stars, we could expect gravity waves to be generated by turbulent motions in the convective core (Denissenkov et al 1999). The momentum will be deposited where the Doppler shift of the waves resulting from differential rotation is equal to the initial wave frequency. From the work by Montalban & Schatzman (1996), we know that in general the deposition of energy decreases very quickly away from the boundaries of a convective zone. The same was found

by Denissenkov et al (1999), who show that uniform rotation sustained by gravity waves is limited to the very inner radiative envelope; the size of the region of uniform rotation enforced by gravity waves likely increases with stellar mass. Only angular momentum may be directly transported by gravity waves and not chemical elements. Nonetheless, the transport of momentum by waves, which reduces the differential rotation, could also indirectly influence the distribution of chemical elements in stars.

2.6 Mass Loss and Rotation

Mass loss by stellar winds is a dominant effect in the evolution of Upper MS stars (Chiosi & Maeder 1986). The mass loss rates currently applied in stellar models are based on the observations of de Jager et al 1988, Lamers & Cassinelli 1996. A significant growth of the mass flux of OB stars with rotation, i.e. by 2–3 powers of 10, was found by Vardya (1985). Nieuwenhuijzen & de Jager (1988) suggested that the correlation found by Vardya mainly reflects the distributions of the mass loss rates $\dot{M}$ and of the rotation velocities $v_{\rm rot}$ over the HR diagram. After trying to disentangle the effects of L, $T_{\rm eff}$, and $v_{\rm rot}$, they found that the $\dot{M}$-rates seem to increase only slightly with rotation for O- and B-type stars. The result by Vardya might not be incorrect; when the data for OB stars by Nieuwenhuijzen & de Jager (1988) are considered, a correlation of the mass fluxes with $v_{\rm rot}$ is noticeable. These authors also point out that the equatorial $\dot{M}$-rates of Be stars are larger by a factor 10^2. Since Be stars are essentially B stars with fast rotation, a single description of the large changes of the $\dot{M}$-rates from the low to the high values of $v_{\rm rot}$ should be considered.

On the theoretical side, Pauldrach et al (1986) and Poe & Friend (1986) found a very weak change of the $\dot{M}$-rates with $v_{\rm rot}$ for O-stars: The increase amounts to about 30% for $v_{\rm rot} = 350$ km/sec. Friend & Abbott (1986) found an increase of the $\dot{M}$-rates, which can be fitted by the relation (Langer 1998, Heger & Langer 1998)

$$\dot{M}(v_{\rm rot}) = \dot{M}(v_{\rm rot} = 0) \left(\frac{1}{1 - \frac{v_{\rm rot}}{v_{\rm crit}}} \right)^{\xi}, \qquad (13)$$

with $\xi = 0.43$; this expression is often used in evolutionary models.

The previous wind models of rotating stars are incomplete because they do not account for the von Zeipel theorem. The gravity darkening at the equator leads to a reduction of the equatorial mass flux (Owocki et al 1996; Owocki & Gayley 1997, 1998). This leads to very different predictions for the wind morphology than those of the current wind-compressed disk model by Bjorkman & Cassinelli (1993), which is currently advocated to explain disk formation. Equatorial disks may form quite naturally around rotating stars, however. The theory of radiative winds, with revised expressions of the von Zeipel theorem and of the Eddington factor, has been applied to rotating stars (Maeder 1999a). There are two main sources of wind anisotropies: (*1*) the $g_{\rm eff}$-effect, which favors polar ejection, since the polar

caps of a rotating star are hotter; and (*2*) the opacity or κ-effect, which favors an equatorial ejection when the opacity is large enough at the equator as a result of an opacity law that increases rapidly with decreasing temperature. In O-type stars, because opacity results mainly from the T-independent electron scattering, the $g_{\rm eff}$ -effect is likely to dominate and to raise a fast, highly ionized polar wind. In B-type and later stars, where a T-growing opacity is present in the external layers, the opacity effect should favor a dense equatorial wind and ring formation, with low terminal velocities and low ionization.

The so-called B[e] stars (Zickgraf 1999) are known to show both a fast, highly ionized polar wind and a slow, dense, low ionized equatorial ejection, and they may be a template of the $g_{\rm eff}$- and κ-effects. At some values of T, the ionization equilibrium of the stellar wind changes rather abruptly, as do the opacity and the force-multipliers that characterize the opacities (Kudritzki et al 1989, Lamers 1997, Lamers 1999). Such transitions, which Lamers calls the bi-stability of stellar winds, may favor strong anisotropies of the winds, and even create some symmetrical rings at the latitude where an opacity peak occurs on the T-varying surface of the star.

It could be thought at first sight that wind anisotropies have no direct consequences for stellar evolution. This is not at all the case. Like magnetic coupling for low-mass stars, the anisotropic mass loss selectively removes the angular momentum (Maeder 1999a) and influences further evolution. Winds through polar caps, as are likely in O-stars, remove very little angular momentum, whereas equatorial mass loss removes considerable angular momentum from the stellar surface.

3. MAIN SEQUENCE EVOLUTION OF ROTATING STARS

3.1 Evolution of Internal Rotation

As a result of transport processes, contraction, and expansion, the stars should be differentially rotating, with a strong horizontal turbulence enforcing a rotation law of the form Ω constant on isobars (Zahn 1992). The whole problem must be treated self-consistently, because differential rotation in turn determines the behaviors of the meridional circulation and turbulence, which themselves contribute to differential rotation. There are various approximations to treat this physical problem (Pinsonneault et al 1989, 1991; Chaboyer et al 1995a,b; Langer 1998; Heger & Langer 1998). In some works, rigid rotation is assumed, whereas in other works advection is treated as a diffusion with the risk that even the sign of the effect is the wrong one! Some authors, in order to fit the observations, introduce several efficiency factors such as f_μ, f_c, and so on. The problem is that the sensitivity of the results to these many efficiency factors is as large, or even larger, than the sensitivity to rotation.

A simplification was applied by Urpin et al (1996), who assumed equilibrium between the outward transport of angular momentum by diffusion and the inward transport by circulation, as was also suggested by Zahn (1992). This is the

stationary case discussed in Section 2.3 for which Equation 4 applies. The values of $U(r)$ are always positive, and the circulation has only one loop. Urpin et al (1996) point out that the stationary distribution of Ω arranges itself so as to reduce $U(r)$ to a minimum value over the bulk of the star. This makes the values of $U(r)$ of the order of $10^{-5}-10^{-6}$ cm/s, which is quite insufficient to produce any efficient mixing in a 20 $M_\odot$ star.

The initial nonstationary approach to equilibrium in 10 and 30 $M_\odot$ stars has been studied by Denissenkov et al (1999). In a very short time—about 1% of the MS lifetime t_{MS}—$\Omega(r)$ converges towards a profile with a small degree of differential rotation and with very small values of $U(r)$ (Urpin et al 1996). The circulation shows two cells, an internal one rising along the polar axis and an external one descending at the pole. The evolution is not calculated, but it is noted that the timescale $t_{\rm circ}$ (which behaves like Ω^{-2}) is very short with respect to the MS lifetime for most Upper MS stars, and that the ratio $\frac{t_{\rm mix}}{t_{MS}} \geq 1$ (Equation 7). It is noticeable that $t_{\rm circ} \ll t_{\rm mix}$, so that no efficiency factors are needed to reduce the mixing of chemical elements compared with the transport of angular momentum. This reduction naturally results from the effect of the horizontal turbulence.

The full evolution of the rotation law has been studied with the nonstationary scheme for a 9 $M_\odot$ star by Talon et al (1997), and for stars from 5 to 120 $M_\odot$ (including the effects of mass loss) by Meynet & Maeder (2000). The very fast initial convergences of $\Omega(r)$ and of $U(r)$ are confirmed. However, after convergence the asymptotic state of $U(r)$ does not correspond to the stationary approximation. In the full solution, $U(r)$ changes sign in the external region and thus transports some angular momentum outward, which is not the case in the stationary solution. Also, contrary to the classical result of the Eddington-Sweet circulation (Equation 8), it is found that $U(r)$ depends very little on the initial rotation.

Figure 1 shows the evolution of $\Omega(r)$ during MS evolution of a 20 $M_\odot$ star. Mass loss at the stellar surface removes a substantial fraction of the total angular momentum, which makes $\Omega(r)$ decrease with time everywhere in the star. The outer zone with inverse circulation progressively deepens during MS evolution, because a growing part of the outer layers has lower densities. This inverse circulation contributes to the outward transport of angular momentum. The deepening of the inverse circulation also has the consequence that the stationary and nonstationary solutions differ more and more as the evolution proceeds, because no inverse circulation is predicted by the stationary solution. This shows that the stationary solutions are too simplified and that outward and inward transport never reach exact equilibrium, contrary to the initial expectations.

Figure 2 shows the various diffusion coefficients inside a 20 $M_\odot$ star when the hydrogen mass fraction at the center is equal to 0.20. We notice that in general $K \geq D_h \geq D_{\rm shear} \geq D_{\rm eff}$. This confirms the basic hypothesis of a large D_h necessary to validate the assumption of shellular rotation.

The characteristic time $t_{\rm mix}$ of the mixing processes is of the same order as the lifetime $t_{\rm H}$ of the H-burning phase for the Upper MS stars (Maeder 1987). Indeed,

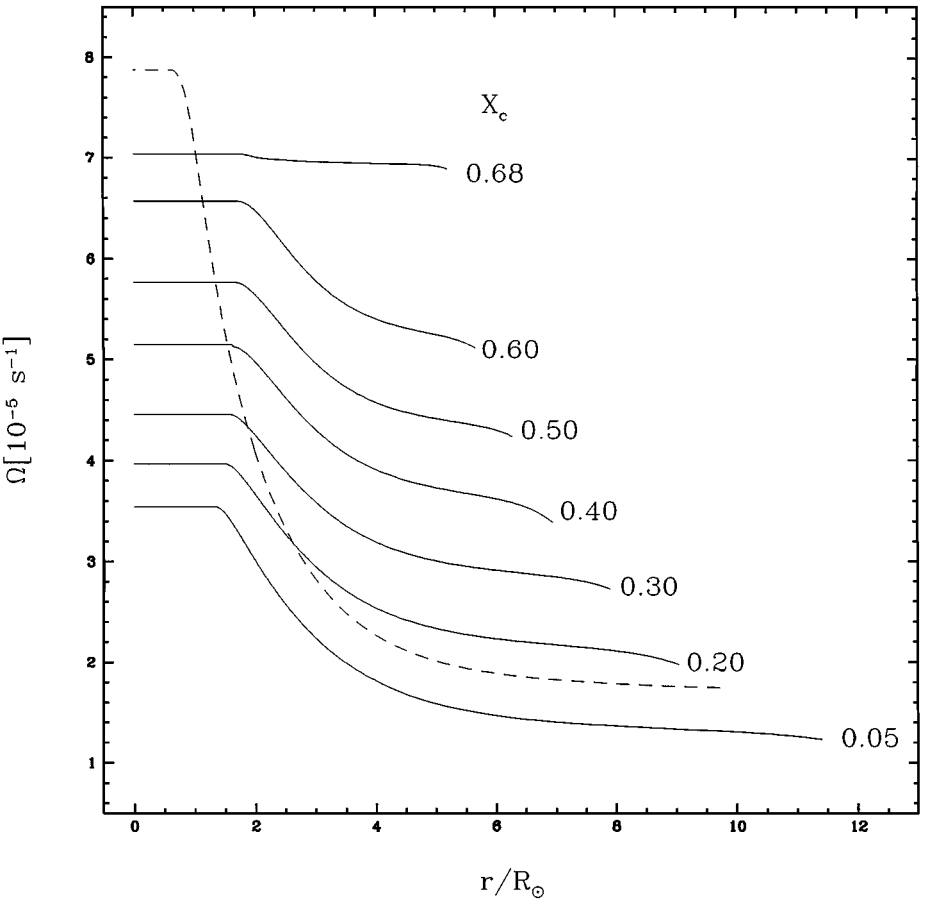

Figure 1 Evolution of the angular velocity Ω as a function of the distance to the center in a 20 $M_\odot$ star with an initial $v_{rot} =$ 300 km/s. X_c is the hydrogen mass fraction at the center. The broken line shows the profile when the He-core contracts at the end of the H-burning phase.

if shear mixing is the dominant mixing process, the timescale is $t_{mix} \simeq \frac{R^2}{D_{shear}}$, and for a given degree of differential rotation it behaves like $t_{mix} \simeq K^{-1}$, which itself goes like $M^{-1.7}$. The timescale t_H behaves like $M^{-0.7}$ for $M \geq 15$ $M_\odot$ (Maeder 1998). Thus, for larger masses t_{mix} tends to decrease much faster than t_H, and mixing processes grow in importance. From the end of MS evolution when $X_c \leq 0.05$, central contraction starts dominating the evolution of the central $\Omega(r)$, which grows quickly until core collapse. During these post-MS phases, the average value of t_{mix} will be longer than the nuclear lifetimes. Thus, the rotational mixing processes during these phases may be globally unimportant (Heger et al 2000, Meynet & Maeder 2000). Nonetheless, it is likely that in some regions of a rotating star in the

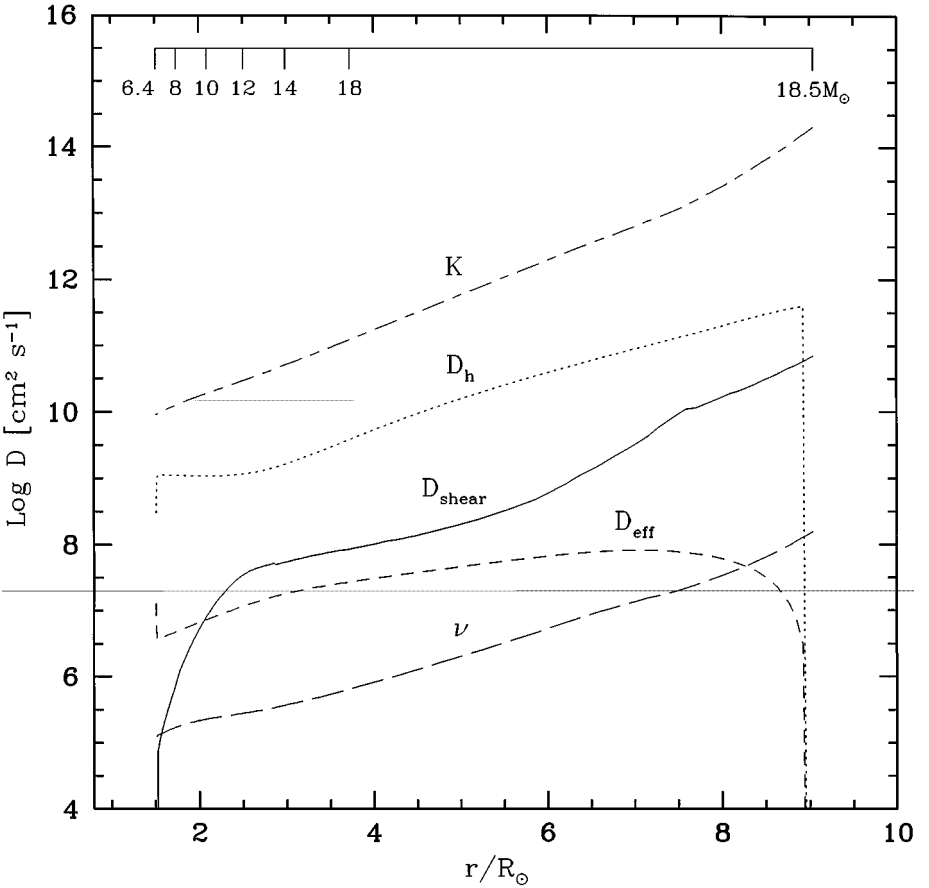

Figure 2 Internal values of K the thermal diffusivity, $D_{\rm h}$ the coefficient of horizontal turbulence, $D_{\rm shear}$ the shear diffusion coefficient, $D_{\rm eff}$ the effective diffusivity (see text) and ν the total viscosity (radiative+molecular) in the radiative envelope of a 20 $M_\odot$ star with an initial $v_{\rm rot} = 300$ km/s. The lagrangian mass coordinate is given on the upper scale. Here, the hydrogen mass fraction at the center $X_c = 0.20$.

advanced stages, the Ω-gradient may become so large as a result of extreme central contraction that some other local instabilities develop, leading to fast mixing.

3.2 Evolution of $V_{\rm rot}$: The Case of Be Stars

The evolution of the surface rotational velocities $v_{\rm rot}$ at the equator is a consequence of the processes discussed in the preceding section. Let us first consider the two extreme cases of coupling and no coupling between adjacent layers, first examined in the early works by Oke & Greenstein (1954) and Sandage (1955): (*1*) the case of rigid rotation and (*2*) the case of local conservation. (*1*) For rigid rotation, $v_{\rm rot}$

remains nearly constant during the MS phase (Fliegner & Langer 1995). This is because the effects of core contraction and envelope expansion nearly compensate for one another. (*2*) For local conservation of the angular momentum we have $v_{\rm rot} = \Omega\, R \sim R^{-1}$, whereas the critical velocity changes like $v_{\rm crit} \sim R^{-\frac{1}{2}}$. Thus, the inflation of the stellar radius R during evolution makes rotation less and less critical. The opposite effect may occur during a blueward crossing of the HR diagram, and then critical rotation may be reached (Section 5.2). Endal & Sofia (1979) have shown that the ratio $v_{\rm rot}(case\ 1)/v_{\rm rot}(case\ 2) \simeq 1.8$ before the crossing of the HR diagram for intermediate mass stars. The truth generally lies between the two cases, closer to the rigid case during the MS phase because transport processes have more time to proceed. In post-MS phases, and in particular during the fast crossings of the HR diagram, the evolution timescale is short, so that little transport occurs and the evolution of $v_{\rm rot}$ closely resembles that of local conservation.

Stars in solid body rotation may reach the breakup limit before the end of the MS phase even for moderate initial $v_{\rm rot}$ (Sackmann & Anand 1970, Langer 1997). However, this is a consequence of the simplified assumption of solid body rotation. With diffusion and transport, it is less easy for the star to reach the breakup limit. For a 20 $M_\odot$ model without mass loss (dotted line in Figures 3 and 4), $v_{\rm rot}$ grows and the ratio $\frac{\Omega}{\Omega_{\rm crit}}$ may become close to 1 before the end of the MS phase. For stars with M<15 $M_\odot$, where mass loss is small, the ratio $\frac{\Omega}{\Omega_{\rm crit}}$ also increases during the MS phase and the breakup or Ω-limit may be reached during the MS phase. If so, the mass loss should then become very intense, until the velocity again becomes subcritical. It is somehow paradoxical that small or no mass loss rates during the bulk of the MS phase (as at low metallicity Z) may lead to very high mass loss at the end of the MS evolution for rotating stars. This may be the cause of some ejection processes as in Luminous Blue Variables (LBV), B[e], and Be stars. We may wonder whether the higher relative number of Be stars observed in lower Z regions (Maeder et al 1999) is simply a consequence of the lower average mass loss in lower metallicity regions, or whether this is related to star formation.

If mass loss is important during MS evolution, then $v_{\rm rot}$ decreases substantially (Figures 3 and 4). Therefore it is not surprising that Be stars, which are likely close to breakup (Slettebak 1966), form not among O-type stars, but mainly among B-type stars, with a relative maximum at type B3. Indeed, to form a Be star it is probably not necessary that the breakup limit be reached exactly. The conditions for an equatorial ejection responsible for the Be spectral features occur when the κ-effect is important (Section 2.6), which requires that the equatorial regions of the rapidly rotating star be below the bi-stability limit. Of course, the higher the rotation, the higher the equatorial mass loss will be.

Any magnetic coupling between the star and the wind would dramatically reduce $v_{\rm rot}$. However, such a coupling does not seem to be important in general, except for Bp and Ap stars. MacGregor et al (1992) show that even in the presence of a small magnetic field of 100 G, the rotation velocities of OB stars should be much lower than observed. This result agrees with that of Mathys (1999), who finds no detectable magnetic field in hot stars.

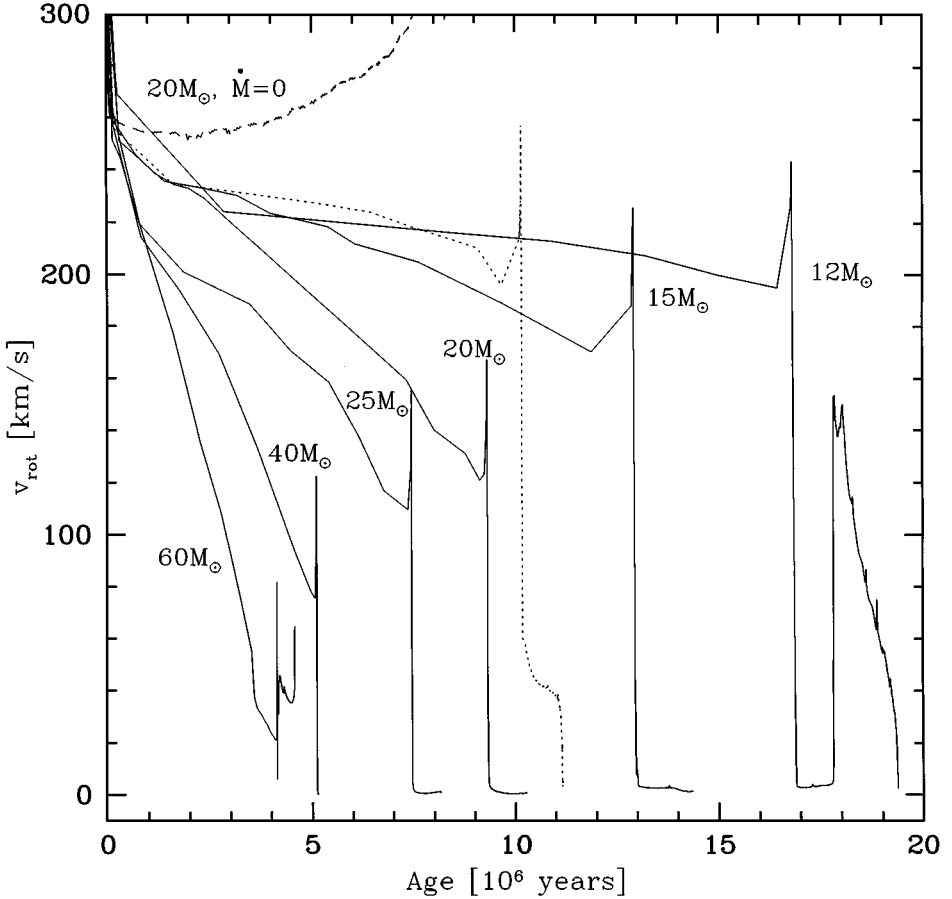

Figure 3 Evolution of the surface equatorial velocity as a function of time for stars of various initial stellar masses (Meynet & Maeder 2000). All models have an initial velocity of 300 km/s. The continuous lines refer to solar metallicity models, the dotted line corresponds to a 20 $M_\odot$ star with Z = 0.004. The dashed line corresponds to a 20 $M_\odot$ star without mass loss.

3.2.1 Effects of Mass Loss on Rotation Mass loss by stellar winds drastically reduces v_{rot} during evolution (Packet et al 1980, Langer & Heger 1998; Figures 3 and 4). Even if isotropic, the stellar winds carry away considerable angular momentum, and this is even more important in the case of equatorial mass loss. The new surface layers then have a lower v_{rot} as a result of expansion and redistribution.

With the simplified assumption of solid body rotation for a 60 $M_\odot$ model with mass loss, Langer (1997, 1998) found a convergence of v_{rot} toward the critical value (the Ω-limit), before the end of the MS phase, for all initial velocities above 100 km/s. The overall result is that the final velocities are the same (all are at the critical

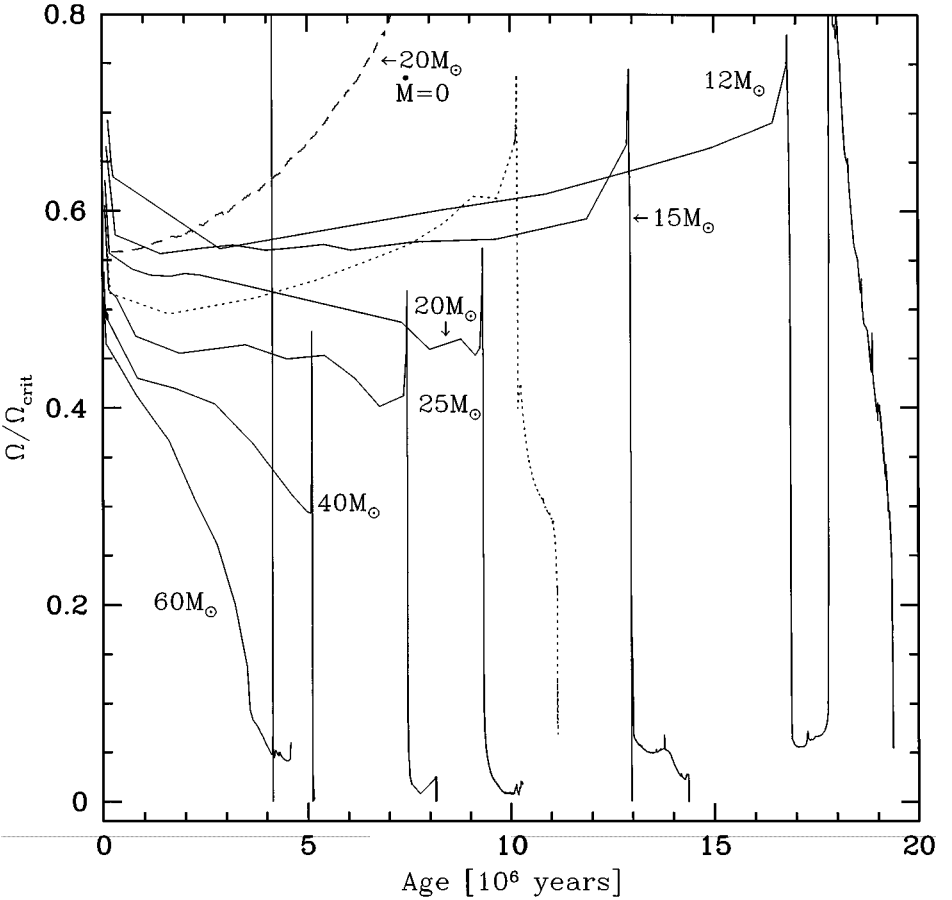

Figure 4 Same as Figure 3 for the ratio Ω/Ω_{crit} of the angular velocity to the break-up velocity at the stellar surface.

limit), whereas the final MS masses strongly depend on the initial rotation. This convergence toward the Ω-limit clearly results also from the simplified assumption of rigid rotation, which grossly exagerates the coupling of the surface layers.

Figure 3 illustrates the decrease in v_{rot} during evolution when the various transport mechanisms are followed in detail. The decrease in v_{rot} is much greater for larger initial stellar masses because mass loss is greater for them. The same is true for $\frac{\Omega}{\Omega_{crit}}$ (Figure 4). For $M \geq 40$ $M_\odot$ the velocities v_{rot} will remain largely subcritical for all initial velocities, except during the overall contraction phase at the end of MS evolution. For a given initial mass, the resulting scatter of v_{rot} should be smaller at the end of the MS phase, but this is not a convergence toward the Ω-limit, as occurs for models with solid body rotation (Langer 1997, 1998). The

final masses are of course lower for greater rotation; because mass loss is enhanced by rotation, this results in a large scatter of masses and $v_{\rm rot}$ at a given luminosity.

3.2.2 Comparison with Observations Only a few comparisons between the observed $v_{\rm rot}$ and the model predictions have been made until now. Conti & Ebbets (1977) found that $v_{\rm rot}$ in O-type giants and supergiants is not as low as they expected from models with rotation conserved in shells. This fact and the relative absence of low rotators among the evolved O-stars led them to conclude that another line-broadening mechanism, such as macroturbulence, should be present in these objects. The same conclusion based on similar arguments was supported by Penny (1996) and Howarth et al (1997). This conclusion needs to be further verified, since the decrease predicted by the new models is not as rapid as for local conservation.

It is well known that the average value of $v_{\rm rot}$ increases from the early O-type to the early B-type stars (Slettebak 1970). This may be the signature of the effect of higher losses of mass and angular momentum in the more massive stars (Penny 1996), which leads to a lower average rotation in the course of the MS phase. We notice that the increase of $v_{\rm rot}$ from O to B stars is larger for the stars of class IV than for the stars of class V (Fukuda 1982), which is expected because the difference resulting from mass loss is more visible near the end of the MS phase (Figure 3). The stars of luminosity class I (Fukuda 1982) show a fast decline of the average $v_{\rm rot}$ from the O-type to the B-type stars. Because the supergiants of class I originate from the most massive stars, which evolve at approximately constant luminosity, this last effect could be related to the fact that for a given initial mass, $v_{\rm rot}$ declines strongly as the star moves away from the MS (Langer 1998).

3.3 The HR Diagram, Lifetimes, and Isochrones

As always in stellar evolution, the shape of the tracks is closely related to the internal distribution of the mean molecular weight μ. All results show that the convective cores are slightly increased by rotation (Maeder 1987, 1998; Langer 1992; Talon et al 1997; Meynet 1998, 1999; Heger et al 2000). The height of the μ- discontinuity at the edge of the core is reduced, and there is a mild composition gradient built up from the core to the surface, which may then be slightly enriched in helium and nitrogen. For low or moderate rotation the convective core shrinks as usual during MS evolution, whereas for high masses ($M \geq 40$ M$_\odot$) and large initial rotations ($\frac{\Omega}{\Omega_{\rm crit}} \geq 0.5$) the convective core grows in mass during evolution. These behaviors, i.e. reduction or growth of the core, determine whether the star will follow respectively the usual redward MS tracks in the HR diagram, or whether it will bifurcate to the blue (cf Maeder 1987, Langer 1992) toward the classical tracks of homogeneous evolution (Schwarzschild 1958) and likely produce W-R stars (Section 5.4). Also, for O- and B-type stars, fast rotation increases the He content of the envelope, and the decrease of the opacity also favors a blueward track.

Figure 5 shows the overall HR diagram for rotating and nonrotating stars. The atmospheric distortions produce a shift to the red in the HR diagram by several 0.01 in (B-V), with only a small change of luminosity, on average (Maeder & Peytremann 1970, Collins & Sonneborn 1977). During MS evolution, the luminosity of the rotating stars grows faster and the tracks extend farther away from the ZAMS, as in the case of a moderate overshooting (Maeder 1987, Langer 1992, Sofia et al 1994, Talon et al 1997). This effect introduces a significant scatter in the mass-luminosity relation (Meynet 1998), in the sense that fast rotators are overluminous with respect to their actual masses. This may explain some of the discrepancies between the evolutionary masses and the direct mass estimates in some binaries (Penny et al 1999). In this context, we recall that for a decade a severe mass discrepancy beween spectroscopic and evolutionary masses was claimed by some authors (Groenewegen et al 1989, Kudritzki et al 1992, Herrero et al 1992). Most of the problem has collapsed and was shown to be a result of the proximity of O-stars to the Eddington limit (Lamers & Leitherer 1993, Herrero et al 1999) and of the large effect of metal line blanketing not usually accounted for in the atmosphere models of massive stars (Lanz et al 1996).

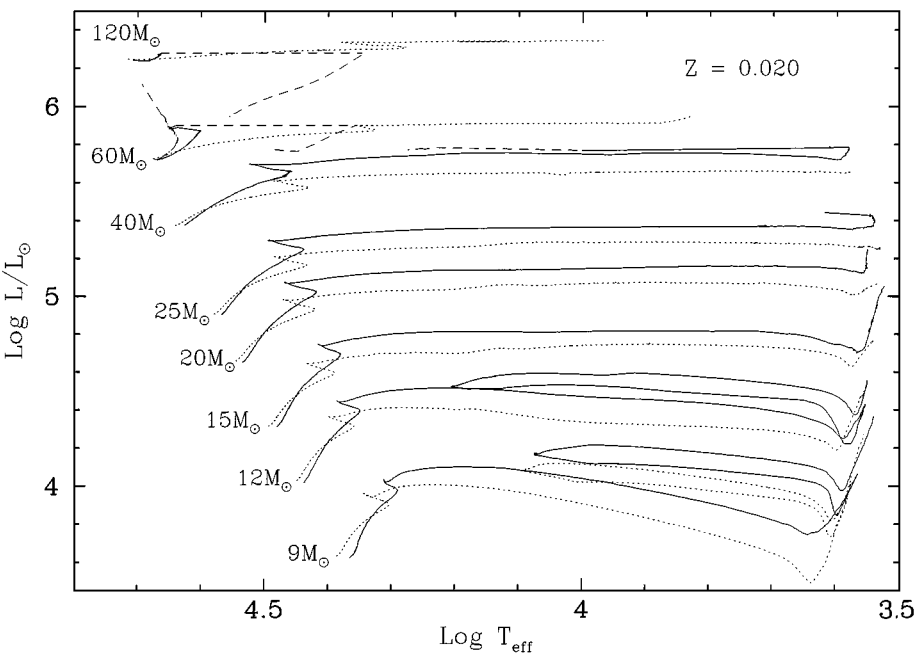

Figure 5 Part of the evolutionary tracks for non-rotating (dotted lines) and rotating (continuous lines) models with solar metallicity (Meynet & Maeder 2000). The rotating models have an initial velocity $v_{\rm rot}$ of 300 km/s. The long dashed track corresponds to a very fast rotating star ($v_{\rm rot} \sim 400$ km/s) of 60 $M_\odot$, which follows a nearly homogeneous evolution. The short dashed tracks indicate the beginning of the W-R phases.

There is little difference between tracks with $v_{\rm rot} = 200$ or 300 km/s (Meynet & Maeder 2000; see also Talon et al 1997). If the effects behaved like $v_{\rm rot}^2$, larger differences would exist. This saturation effect occurs because outward transport of angular momentum by shears is larger when rotation is larger; also, a larger rotation produces more mass loss, which further reduces rotation during evolution.

For the model of 12 $M_\odot$, a blue loop appears when rotation is included. This results from the smaller core in the rotating model, because in this model the growth of the core is prevented by a very large external convective zone. Thus, rotation not only modifies the mass-luminosity relation for Cepheids, but also it increases the maximum possible luminosity for the occurrence of Cepheids.

3.3.1 Lifetimes and Isochrones The lifetimes $t_{\rm H}$ in the H-burning phase grow only moderately because more nuclear fuel is available, but at the same time the luminosity is larger. The net result is an increase by about 20% to 30% for an initial velocity of 200 km/s (Talon et al 1997, Meynet & Maeder 2000). This influences the isochrones and age determinations. For example, for $v_{\rm rot} = 200$ km/s, the isochrone of log age $= 7.0$ is the same as that of log age $= 6.90$ without rotation (Meynet 2000). Thus, accounting for rotation could lead to ages larger by about 25% for O- and early B-type stars. However, since the cluster ages are generally determined on the basis of the blue envelope of the observed sequence, where most low rotators lie (Maeder 1971), it is likely that the effect of rotation in current age determinations is rather small. If a blueward track occurs, the larger core and mixing lead to much longer lifetimes in the H-burning phase. In this case, the fitting of timelines becomes hazardous.

4. ROTATION AND CHEMICAL ABUNDANCES

4.1 Observations

Chemical abundances are a very powerful test of internal evolution, and they give strong evidence in favor of some additional mixing processes in O- and B-type stars, in supergiants, and in red giants of lower masses.

4.1.1 Abundances in MS O- and B-Type Stars Much evidence of He and N excesses in O-type and early B-type stars have been reported over the last decade (Gies & Lambert 1992; Herrero et al 1992, 1998; Kilian 1992; Kendall et al 1995, 1996; Lyubimkov 1996, 1998). We can extract the following main points:

1. The OBN stars show significant He and N excesses. OBN stars are more frequent among stars above 40 $M_\odot$ (Walborn 1988, Schönberner et al 1988, Herrero et al 1992).
2. All fast rotators among the O-stars show some He excesses (Herrero et al 1992, 1998, 1999; Lyubimkov 1996).

3. Although rather controversial initially, there seems to be an increase of the He and N abundances with relative age (i.e. the fraction t/t_{MS} of the MS lifetime spent) for the early B-type stars (Lyubimkov 1991, 1996; Gies & Lambert 1992, see note added in proof; Denissenkov 1994). Lyubimkov (1996) suggests a sharp rise from $(He/H) = 0.08$–0.10 to 0.20 in number for O-stars when $t/t_{MS} \geq 0.5-0.7$, whereas for B-type stars the corresponding value rises to 0.12–0.14. As for nitrogen, its abundance is estimated to rise to about 3 times for a 14 $M_\odot$ and 2 times for a 10 $M_\odot$ star. An increase of the N abundance by a factor of 2–3 for an O-star with the average v_{rot} of 200 km/s is the order of magnitude typically considered as a constraint for recent stellar models (Heger et al 2000).
4. The boron abundances in five B-stars on the MS were found to be smaller than the cosmic meteoritic value by a factor of at least 3 or 4 (Venn et al 1996). Boron depletion occurs in stars that also show N excess; this supports the idea that rotational mixing occurs throughout the star (Fliegner et al 1996).

4.1.2 Abundances in Supergiants The main observations are as follows:

1. He and N excesses seem to be the rule among OB supergiants (Walborn 1988). According to Walborn, only the small group of the "peculiar" OBC stars has the normal cosmic abundances. An excess of He, sometimes called the "helium discrepancy," and corresponding excesses of N have been found by a number of authors (Voels et al 1989; Lennon et al 1991; Gies & Lambert 1992; Herrero et al 1992, 1999; Smith & Howarth 1994; Venn 1995a,b; Crowther 1997; McEarlean 1998; McEarlean et al 1999). As shown by these last authors, the determination of the helium abundance also depends on the adopted value for microturbulence. However, Villamariz & Herrero (1999) and Herrero et al (1999) point out that the helium discrepancy is only reduced, not solved, when microturbulence is accounted for.
2. Evidence of highly CNO-processed material is present for B supergiants in the range 20– 40 $M_\odot$, (McEarlean et al 1999). Values of [N/H] (i.e. the difference in log with respect to the solar values) amounting to 0.6 dex have been found for B supergiants around 20 $M_\odot$ (Venn 1995a,b). Such values agree with the enrichments found in the ejecta of SN 1987A (Fransson et al 1989).
3. The values of [N/H] for galactic A-type supergiants around 12 $M_\odot$ lie between 0 and 0.4 dex (Venn 1995a,b, 1999). All of these values are globally consistent with the preceding results from Lyubimkov (1996). Takeda & Takada-Hidai (1995) have suggested that these excesses are greater for larger masses, a result in agreement with theory and also recently confirmed by McEarlean et al (1999). For the A-type supergiants

in the SMC, the N/H excesses are much larger, spanning a range of [N/H] = 0 to 1.2 dex (Venn 1998; Venn 1999).

4. Na excesses have been found in yellow supergiants (Boyarchuk & Lyubimkov 1983), and the overabundances seem to be larger for higher-mass stars (Sasselov 1986). Two different explanations have been proposed—one based on the reaction ^{22}Ne(p,γ)^{23}Na (Denissenkov 1994), and the other one based on ^{20}Ne(p,γ)^{21}Na (Prantzos et al 1991), with some additional mixing processes in both cases. The latter reaction seems to have a too-low rate, whereas the first one may work (Denissenkov 1994). The important point is that the observed Na excesses imply some mixing from the deep interior to the surface.
5. Very few abundance determinations exist in yellow and red supergiants. Some excesses of N with respect to C and O have been found by Luck (1978). Barbuy et al (1996) found both N enrichments and normal compositions among the slow rotating F-G supergiants. Isotopic ratios ^{13}C/^{12}C, ^{17}O/^{16}O, and ^{18}O/^{17}O for red supergiants would provide very useful information. However, the dilution factor in the convective envelope of red giants and supergiants is so large that it is not possible from the rare data available to draw any conclusions about the presence of additional mixing (Maeder 1987, Dearborn 1992, Denissenkov 1994, El Eid 1994).

4.2 Comparisons of Models and Observations

4.2.1 Massive Stars in MS and Post-MS Phases Let us first recall that from the comparison of $t_{\rm mix}$ and $t_{\rm H}$, it is clear that mixing processes are more efficient in more massive stars. For the intermediate-mass stars of the B and A types, no global mixing is currently predicted. Often, the comparisons with the observed abundance excesses for O- and B-type stars are used to adjust some efficiency factors in the models (Pinsonneault et al 1989, Weiss et al 1988, Weiss 1994, Chaboyer et al 1995a,b, Heger et al 2000). Although not fully consistent, these approaches help us appreciate the importance of the various possible effects. The old prescriptions of Zahn (1983) were applied by Maeder (1987), Langer (1992), and Eryurt et al (1994), and led to some surface He and N enrichments.

The prescriptions by Zahn (1992) were applied to the evolution of a 9 $M_\odot$ star (Talon et al 1997). These last authors found essentially no He enrichment and a moderate enhancement (factor $\sim$2) of N at the stellar surface, for an initial velocity of 300 km/s. Figure 6 illustrates the changes of the N/H ratios from the ZAMS to the red supergiant stage for 20 and 25 $M_\odot$ stars (Meynet & Maeder 2000). For non-rotating stars, the surface enrichment in nitrogen occurs only when the star reaches the red supergiant phase; there, CNO elements are dredged up by deep convection. For rotating stars, N excesses occur already during the MS phase, and they are larger for high rotation and initial stellar masses. At the end of the MS phase, for solar metallicity Z = 0.02, the predicted excesses

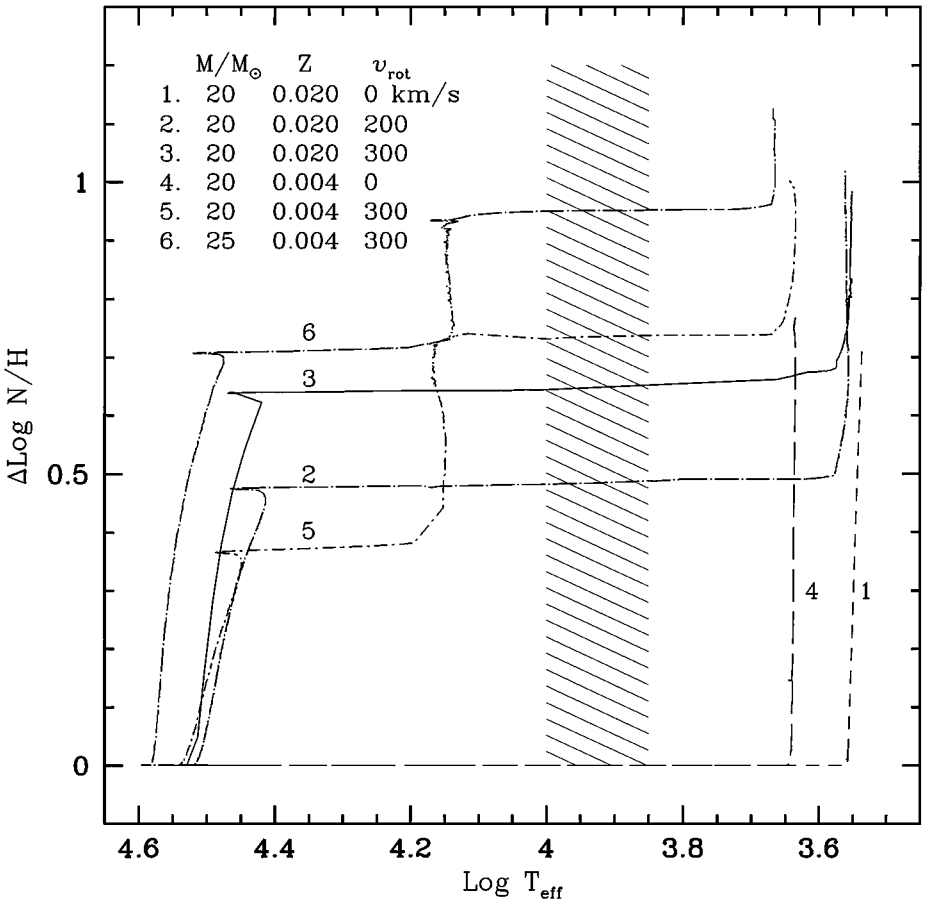

Figure 6 Evolution as a function of log $T_{\rm eff}$ of $\Delta \log \frac{N}{H} = \log(N/H) - \log(N/H)_i$, where N and H are the surface abundances (in number) of nitrogen and hydrogen respectively, the index i indicates initial values. The initial masses, metallicities and rotational velocities are indicated. The shaded area corresponds to the range of observed values (Venn 1999) for A-type supergiants in the SMC.

amount to factors of 3 and 4 for initial $v_{\rm rot} = 200$ and 300 km/s, respectively. At lower metallicity, the N enrichment during the MS phase is smaller, probably because of lower mass loss; however, there is a very large increase (up to a factor of $\sim$10) for late B-type supergiants, because the star spends a lot of time in the blue phase, and mixing processes have time to work. The predictions of Figure 6 agree with the observed excesses for galactic B- and A-type supergiants (Venn 1995a,b, Venn 1998). Also, the very large excesses observed for A-type supergiants in the SMC (Venn 1998, 1999) are remarkably well accounted for.

4.2.2 Questions About Nitrogen Many studies of galactic halo stars, blue compact galaxies, and highly redshifted galaxies have revealed the need for initial production of primary N in addition to the currently accepted mechanism of secondary nitrogen (cf Edmunds & Pagel 1978, Matteucci 1986, Pettini et al 1995, Thuan et al 1995, Centurion et al 1998, Pilyugin 1999, Henry & Worthey 1999). The early production of N in the evolution of galaxies seems to imply that some N is produced in massive stars (Matteucci 1986, Thuan et al 1995). The problem is that the usual stellar models do not show such a production without ad hoc assumptions. Models of rotating stars allow us to clearly identify the conditions for the production of primary N: The star must have an He-burning core and a thick and long-lived H-burning shell, and then diffusion and transport of new ^{12}C from the core to the shell may generate some primary ^{14}N. W-R stars do not seem favorable because the H-shell does not live long enough—it is quickly extinguished and removed by mass loss. Low-metallicity supergiants that have not suffered large mass loss are very favorable sites, especially if rotation is faster at low metallicities.

4.3 Red Giants and AGB Stars

MS stars in the range of 1.5 to $\sim$10 $M_\odot$ show no evidence of extra-mixing; however, there are interesting indications for red giants. The study of $^{12}C/^{13}C$ in cluster red giants (Gilroy 1989) shows that stars between 2.2 $M_\odot$ and 7 $M_\odot$ have ratios close to the standard predictions without mixing. However, red giants below 2.2 $M_\odot$ show $^{12}C/^{13}C$ ratios much lower than the predictions, indicating some extra-mixing (Gilroy 1989; see also Harris et al 1988); the lower the mass, the higher the mixing. On the red giant branch of M67, there are indications of extra-mixing for stars brighter than $\log L/L_\odot \simeq 1.0$, where the first dredge-up occurs (Gilroy & Brown 1991).

From the data on M67, it appears that extra-mixing is only efficient when the H-burning shell reaches the μ-discontinuity left by the inward progression of the outer convective zone (Charbonnel 1994). Prior to this stage, the μ-gradient created by the first dredge-up acts as a barrier to any mixing below the convective envelope (Charbonnel et al 1998). The μ-gradient necessary to prevent mixing is found to be in agreement with that expected to stop the meridional circulation. For stars with $M \geq 2.2$ $M_\odot$, helium ignition occurs in nondegenerate cores, i.e. early enough so that the H-shell does not reach the border left by the outer convective zone and there is always a μ-gradient high enough to prevent mixing (Charbonnel et al 1998). Boothroyd & Sackmann (1999) confirm that extra-mixing and the associated CNO nuclear processing (cool bottom processing, CBP) occur when the H-burning shell erases the μ-barrier established by the first dredge-up, and they predict that the effects of the CBP behave like M^{-2} and Z^{-1}. Further observations of red giants with various masses are very much needed to confirm the relative absence of enrichment for masses ≥ 2.2 $M_\odot$.

For the more advanced stages of intermediate mass stars, the critical questions concern nucleosynthesis and the processes leading to the production of the s-elements in AGB stars (Iben 1999). Rotation appears to allow the formation of larger degenerate cores (Sackmann & Weidemann 1972, Maeder 1974); then, the C/O core mass is further increased during the early AGB phases (Dominguez et al 1996). The large Ω-gradients between the bottom of the convective envelope and the H-burning shell can drive mixing, mainly through the GSF instability and to a lesser extent through shear and meridional circulation between the H- and ^{12}C-rich layers during the third dredge-up in AGB stars (Langer et al 1999b). The neutron production by $^{13}C(\alpha,n)^{16}O$ between the thermal pulses favors the production of s-elements. In further studies on the role of rotation in AGB stars, the exact treatment of the instabilities in regions of steep Ω- and μ-gradients will play a crucial role.

5. POST-MS EVOLUTION WITH ROTATION

The post-MS evolution of rotating stars differs from that of nonrotating stars for three main reasons: (*1*) The structure at He-ignition is different because of the rotationally induced mixing during the previous H-burning phase; in rotating stars, the He cores are more massive (Sreenivasan & Wilson 1985b, Sofia et al 1994) and the radiative envelope is enriched with CNO-burning products (Maeder 1987, Heger et al 2000, Meynet & Maeder 2000); (*2*) The mass loss rates are increased by rotation (Friend & Abbott 1986, Langer 1998; Section 2.6); and (*3*) Rotational transport mechanisms may also operate in the interior during the post-MS phases. In massive stars, however, the timescales for mixing and circulation, $t_{\rm mix}$ and $t_{\rm circ}$, are much larger than the evolutionary timescale by one to two orders of magnitude during the He-burning phase (Endal & Sofia 1978) and even larger in the post–He-burning phases (Heger et al 2000). Thus, these processes will have small global effects during these stages. However, because of very high angular velocity gradients occuring locally, some instabilities may appear on much smaller timescales (Endal & Sofia 1978, Deupree 1995).

5.1 Internal Effects

The fast contraction of the core and expansion of the envelope that follow the end of the MS phase produce an acceleration of Ω in the inner regions and a slowing down in the outer layers (Kippenhahn et al 1970, Endal & Sofia 1978, Talon et al 1997, Heger et al 2000, Meynet & Maeder 2000). Typically, for a 20 $M_\odot$ model with an initial $v_{\rm rot} = 300$ km/s (Figure 5), the ratio of the central to surface angular velocity never exceeds 5 during the MS phase, whereas it increases to 10^5 or 10^6 during the He-burning phase (Section 5.5).

At the beginning of the He-burning phase, the He cores in rotating models are more massive by about 15% for $v_{\rm rot} = 300$ km/s. The further evolution of the

convective core depends on the adopted criterion for convection. If the Ledoux criterion is used, the growth of the convective core is prevented by the μ-barriers and remains small. Above it, several small convective zones appear, each separated by semiconvective layers (e.g. Langer 1991c). If the Schwarzschild criterion is used, the convective core simply grows in mass. For both cases, the rotational effects depend on their sensitivity to the μ-gradients. For example, models with the Ledoux criterion show that when rotational mixing is artificially made insensitive to μ-gradients, the shear mixing operates efficiently in semiconvective regions and considerably enlarges the final C/O core masses (Heger et al 2000). Typically, the C/O core mass increases from a value of 1.77 $M_\odot$ in the 15 $M_\odot$ nonrotating model to a value of 3.4 $M_\odot$ for an initial $v_{\rm rot} = 200$ km/s. For a similar rotating model using the Schwarzschild criterion and incorporating the inhibiting effect of the μ-gradients, Meynet & Maeder (2000) obtained a C/O core mass of 2.9 $M_\odot$, to be compared with the value of 2 $M_\odot$ obtained in the nonrotating model. The treatment of the μ-gradient is thus critical, because the C/O core masses play a key role in determining the stellar remnants as well as the chemical yields (Section 5.5).

5.2 Evolution in the HR Diagram, Lifetimes, and Rotational Velocities

Rotating as well as nonrotating models with initial masses between 9 and 40 $M_\odot$ at solar metallicity evolve toward the red supergiant (RSG) stage after the MS phase (Kippenhahn et al 1970, Sofia et al 1994, Heger 1998, Meynet & Maeder 2000). Because of the larger He cores, the rotating stars have higher luminosities, as long as mass loss is not too large. The initial distribution of the rotational velocities will thus introduce some scatter in the luminosities of the supergiants originating from the same initial mass. The lower the sensitivity of the mixing processes to the μ-gradients, the greater the scatter. For initial $v_{\rm rot}$ between 0 and 300 km/s, the difference will be of the order of 0.25 mag (Figure 5).

In rotating stars of initial mass between 20 and 40 $M_\odot$, because of the large cores, the quantity of nuclear fuel is larger, but the luminosities are also higher and thus the He-burning lifetimes change slightly; as an example, for initial $v_{\rm rot} =$ 200–300 km/s, the changes are less than 5%. The ratios $t_{\rm He}/t_{\rm H}$ of the He to H-burning lifetimes are not very sensitive to rotation and remain around 10% (Heger 1998, Meynet & Maeder 2000).

5.2.1 The Number Ratio of Blue to Red Supergiants The variation with metallicity Z of the number of blue and red supergiants (RSG) is important in relation to the nature of the supernova progenitors in different environments (cf Langer 1991b,c) and population synthesis (e.g. Cervino & Mas-Hesse 1994, Origlia et al 1999). The observations show that the number ratio (B/R) of blue to red supergiants increases steeply with Z. Cowley et al (1979) examined the variation of the B/R ratio across the Large Magellanic Cloud (LMC) and found that it increases by a factor

of 1.8 when the metallicity is larger by a factor of 1.2. For M_{bol} between -7.5 and -8.5, the B/R ratio is up to 40 or more in inner Galactic regions and only about 4 in the SMC (Humphreys & McElroy 1984). A difference in the B/R ratio of an order of magnitude between the Galaxy and the Small Magellanic Cloud (SMC) was also found from cluster data (Meylan & Maeder 1982). Langer & Maeder (1995) compared different stellar models with the observations and concluded that most massive star models have problems reproducing this observed trend.

Part of this difficulty certainly arises from the fact that supergiants are often close to a neutral state between a blue and a red location in the HR diagram. Even small changes in mass loss, in convection or other mixing processes, greatly affect the evolution and the balance between the red and the blue locations (Stothers & Chin 1973, 1975, 1979, 1992a,b; Maeder 1981; Brunish et al 1986; Maeder & Meynet 1989; Arnett 1991; Chin & Stothers 1991; Langer 1991b,c, 1992; Salasnich et al 1999). As stated by Kippenhahn & Weigert (1990), "the present phase is a sort of magnifying glass, revealing relentlessly the faults of calculations of earlier phases."

The choice of the criterion for convection plays a key role, particularly when the mass loss rates are small. Models with the Ledoux criterion, with or without semiconvection, predict at low metallicity (Z between 0.002 and 0.004) both red and blue supergiants. However, when the metallicity increases, the B/R ratio decreases in contradiction with the observed trend (Stothers & Chin 1992a, Brocato & Castellani 1993, Langer & Maeder 1995). Models with the Schwarzschild criterion, with or without overshooting, can more or less reproduce the observed B/R ratio in the solar neighborhood. However, they predict very few or no red supergiants at the metallicity of the SMC, whereas many are observed (Brunish et al 1986, Schaller et al 1992, Bressan et al 1993, Fagotto et al 1994).

When the mass loss rates are low (i.e. at low Z), a large intermediate convective zone forms in the vicinity of the H-burning shell, homogenizing part of the star and maintaining it as a blue supergiant (Stothers & Chin 1979, Maeder 1981). For larger mass loss rates, the intermediate convective zone is drastically reduced, and the formation of RSG is favored. A further increase of the mass loss rates may bring the star back to the blue. When the He core encompasses more than some critical mass fraction q_c of the total mass (Chiosi et al 1978, Maeder 1981), the star moves to the blue and becomes either a blue supergiant or a W-R star (e.g. Schaller et al 1992, Salasnich et al 1999, Stothers & Chin 1999). The critical mass fraction q_c is equal to 67% at 60 $M_\odot$, 77% at 30 $M_\odot$, and 97% at 15 $M_\odot$ (Maeder 1981). This agrees with the investigations made for lower masses by Giannone et al (1968).

Rotation mainly affects the B/R ratio through its effect on the interior structure and on the mass loss rates. Maeder (1987), Sofia et al (1994), and Talon et al (1997) showed that the effect of additional mixing caused by rotational instabilities in some respect mimics that of a small amount of convective overshoot, which does not favor the formation of RSG at low Z. However, fast rotation also implies higher

mass loss rates by stellar winds, and in general this favors the formation of RSG. In view of these two opposite effects, it is still uncertain whether rotation may solve the B/R problem. Because of the initial distribution of rotational velocities, one expects a scatter of the mass loss rates and therefore different evolutionary scenarios for a given initial mass star (Sreenivasan & Wilson 1985a). However, by producing high mass loss rates even at low metallicity, rotation may help resolve the B/R problem.

Is rotation responsible for the observed characteristics of the blue progenitor of the SN 1987A? The presence of the ring structures around SN 1987A (Burrows et al 1995, Meaburn et al 1995), which likely result from axisymmetric inhomogeneities in the stellar winds ejected by the progenitor (Eriguchi et al 1992, Lloyd et al 1995, Martin & Arnett 1995), and the high level of nitrogen enhancements in the circumstellar material (Fransson et al 1989, Panagia et al 1996, Lundqvist & Fransson 1996) are features that may be explained at least in part by rotation. Woosley et al (2000) suggest that any mechanism that reduces the helium core while simultaneously increasing helium in the envelope would favor a blue supernova progenitor.

5.2.2 Evolution of Surface Velocities As we already stated in Section 3.2, when the star evolves from the blue toward the RSG stage, surface velocities quickly decrease (Endal & Sofia 1979, Langer 1998). For the stars shown in Figure 5, velocities between 20 and 50 km/s are obtained when $\log T_{\rm eff} = 4.0$. Values of the order of 1 km/s are reached at the RSG stage. Observations confirm this rapid decline of surface velocities (Rosendhal 1970, Fukuda 1982). The values at $\log T_{\rm eff} = 4.0$ are in good agreement with Verdugo et al's (1999) recent determinations of rotational velocities for galactic A-type supergiants.

When the star evolves back to the blue from the RSG stage, as is the case for the rotating 12 $M_\odot$ model shown in Figure 5, the rotational velocity approaches the breakup velocity (Heger & Langer 1998, Meynet & Maeder 2000). This behavior results from the stellar contraction which concentrates a large fraction of the angular momentum of the star (previously contained in the extended convective envelope of the RSG) in the outer few hundredths of a solar mass. At the maximum extension of the blue loop, the equatorial velocity at the surface of the 12 $M_\odot$ star (Figure 5) reaches values as high as 150 km/s. As the star evolves back toward the RSG stage, the surface velocity declines again to about 2 km/s. When the star crosses the Cepheid instability strip, its surface velocity is between 10 and 20 km/s, well inside the observed range (Kraft et al 1959, Kraft 1966, Schmidt-Kaler 1982).

The increase in the surface velocity occurs every time a star leaves the Hayashi line to hotter zones of the HRD (Heger & Langer 1998). In most cases, there is observational evidence for axisymmetric circumstellar matter: disks around T Tauri stars during pre-Main-Sequence evolution (e.g. Guilloteau & Dutrey 1998), bipolar planetary nebulae (e.g. Garcia-Segura et al 1999), structures around SN 1987A (e.g. Meaburn et al 1995), and rings around W-R stars (e.g. Marston 1997).

5.3 The Ω, Γ Limits and the LBVs

In recent years, the problem of the very luminous stars close to the Eddington limit and reaching the breakup limit (Langer 1997, 1998) has been discussed in relation to the Luminous Blue Variables (LBVs) and their origin (see Davidson et al 1989, de Jager & Nieuwenhuijzen 1992, Nota & Lamers 1997). The LBVs, also called the Hubble-Sandage Variables and S Dor Variables, are extreme OB supergiants with $\log L/L_\odot \simeq 6.0$ and $T_{\rm eff}$ between about 10,000 and 30,000 K (Humphreys 1989). Only a few of them are known in the Milky Way; among them is η Carinae (Davidson & Humphreys 1997, Davidson et al 1997). LBVs experience giant outbursts with shell ejections. Often they show surrounding bipolar nebulae (Nota et al 1997). Many models and types of instabilities have been proposed to explain the LBV outbursts (de Jager & Nieuwenhuijzen 1992; Stothers & Chin 1993, 1996, 1997; Nota & Lamers 1997).

5.3.1 Physics of the Breakup Limit The first problem concerns the expression of the breakup limit for stars close to the Eddington limit, i.e. for the brightest supergiants. When the radiation field is strong, the radiative acceleration $\vec{g_{\rm rad}}$ must be accounted for in the total acceleration

$$\vec{g_{\rm tot}} = \vec{g_{\rm grav}} + \vec{g_{\rm rot}} + \vec{g_{\rm rad}} = \vec{g_{\rm eff}} + \vec{g_{\rm rad}}, \qquad (14)$$

with a modulus $g_{\rm rad} = (\kappa L/4\pi cR^2)$, where R is the equatorial radius. Thus, the breakup velocity obtained when $\vec{g_{\rm tot}} = 0$ is found to be $v^2_{\rm crit} = \frac{GM}{R}(1-\Gamma)$ (Langer 1997, 1998; Langer & Heger 1998; Lamers 1997), where Γ is the Eddington factor $\Gamma = \kappa L/(4\pi cGM)$. For the most luminous stars, $\Gamma \rightarrow 1$, and thus the critical velocity tends toward zero. This has led Langer (1997, 1998) to conclude that for any initial rotation, the critical limit is reached before the Eddington limit. Therefore, Langer claims that we should speak of an Ω-limit for LBV stars, rather than a Γ-limit.

Glatzel (1998) suggested that the Ω-limit is an artifact resulting from the absence of von Zeipel's relation in the expression of $g_{\rm rad}$. Indeed, with von Zeipel's relation the radiative flux tends toward zero when the resulting gravity is zero. Thus, the critical velocity is just $v^2_{\rm crit} = \frac{GM}{R}$, while rotation reduces (up to 40%; Glatzel 1998) the limiting luminosity. Stothers (1999) also considered that fast rotation reduces the limiting luminosity.

For stars close to the Eddington limit, convection may develop in the outer layers (Langer 1997, Glatzel & Kiriakidis 1998). This is not an objection to the application of the von Zeipel theorem, however, since most of the flux is carried by radiation at the surface. A possible objection though (Langer et al 1999a) is that, according to a generalization of the von Zeipel theorem by Kippenhahn (1977), the radiative flux at the equator may be reduced or increased depending on the internal rotation law. However, the deviations from von Zeipel's theorem are negligible in the current cases of models with shellular rotation (Maeder 1999a). Thus, a study

of the physical conditions, the critical velocity, and the instabilities in rotating stars close to the Eddington limit is still necessary.

5.3.2 The Evolution of LBVs According to the evolutionary models at high masses (Schaller et al 1992, Stothers & Chin 1996, Salasnich et al 1999), there are three possible ways for very massive stars to reach the Ω-limit in the HR diagram:

1. Stars with very large initial mass and high rotation, especially if their $v_{\rm rot}$ is increased by blueward evolution during the MS phase, may reach the Ω-limit in the blue part of the HR diagram. Some fast rotators may reach the breakup limit during the overall contraction phase at the end of the MS, as shown for the 60 $M_\odot$ (Figure 4). If the mass loss for O-stars is mainly bipolar (Maeder 1999a), the reduction of $v_{\rm rot}$ during the MS phase may be smaller. For smaller mass loss rates, as in lower-metallicity galaxies, $v_{\rm crit}$ could possibly be reached earlier in evolution. The star η Carinae shows evidence that the Ω-limit is reached in the blue, and it is likely at the end of its MS phase or beyond in view of its surface composition (Davidson et al 1986, Viotti et al 1989).
2. After the end of the MS phase, when the star evolves redward in the HR diagram, the value of $\frac{\Omega}{\Omega_{\rm crit}}$ becomes quite small because the star evolves with essentially local conservation of angular momentum. Thus, rotation is less important. However, the Γ-limit without rotation lies at a much lower luminosity there (Lamers 1997, Ulmer & Fitzpatrick 1998), so the Ω-limit may be reached by the very massive stars during their redward crossing of the HR diagram.
3. When stars leave the red supergiant phase, either on blue loops or evolving toward the W-R stage, the ratio $\frac{\Omega}{\Omega_{\rm crit}}$ increases significantly. This is caused by conservation of angular momentum in retreating convective envelopes, which contributes to accelerate the rotation of the blueward evolving stars (Heger & Langer 1998). Thus, the Ω-limit may also be reached from the red side. This possibility is particularly interesting because the observed CNO abundances in some nebulae around LBV stars are the same as in red supergiants, which suggests that some LBV may originate from red supergiants (Smith 1997). A similar conclusion was obtained by Waters (1997), who found evidence in some LBV nebulae of crystalline forms of silicates, with composition similar to that of red supergiants.

5.3.3 The Nebulae Around LBVs: Signature of Rotation? Almost all nebulae around LBV stars show a bipolar structure (Nota et al 1995, Nota & Clampin 1997), which may be related to binarity (Damineli 1996, Damineli et al 1997). Most models invoke collisions of winds of different velocities and densities, emitted at different phases of their evolution. In some cases, an equatorial density enhancement is assumed before the outburst (Frank et al 1995; see also Nota et al 1995), whereas other models assume rather arbitrary nonspherical winds or a

ring-like structure interacting with a previous spherical wind (Dwarkadas & Balick 1998, Frank et al 1998). The models by Garcia-Segura et al (1996, 1997) and Langer et al (1999) consider three phases in the formation of the nebula for η Carinae. In both the pre- and post-outburst phases, the star has the spherical fast and low density wind typical of a blue supergiant. At the breakup limit, the star is assumed to have a slow dense wind concentrated in the equatorial plane. The bipolar structure then arises because the shell ejected in the third phase expands more easily into the lower density at the pole. Langer et al (1999) assumed that the equatorial enhancement during the outburst results from the wind-compressed disk model (Bjorkman & Cassinelli 1993), which does not apply if the von Zeipel theorem is used (Owocki & Gayley 1997, 1998). Nevertheless, we note that because of the κ-effect at the breakup limit (Maeder 1999a), a strong equatorial ejection occurs quite naturally and is characterized by a high density and a low velocity, as is required by the colliding wind model of Langer et al (1999).

5.4 Rotation and W-R Star Formation

5.4.1 Generalities Recent reviews on the Wolf-Rayet (W-R) phenomenon have been presented by Abbott & Conti (1987), van der Hucht (1992), Maeder & Conti (1994), and Willis (1999). Wolf-Rayet stars are bare cores of initially massive stars (Lamers et al 1991). Their original H-rich envelope has been removed by stellar winds or through a Roche lobe overflow in a close binary system. Observationally, most W-R stars appear to originate from stars initially more massive than about 40 $M_\odot$ (Conti et al 1983, Conti 1984, Humphreys et al 1985, Tutukov & Yungelson 1985); however, a few stars may originate from initial masses as low as 15–25 $M_\odot$ (Thé et al 1982, Schild & Maeder 1984, Hamann et al 1993, Hamann & Koesterke 1998a, Massey & Johnson 1998). The stars enter the W-R phase as WN stars, i.e. with surface abundances representative of equilibrium CNO processed material. If the peeling off proceeds deep enough, the star may enter the WC phase, during which the He-burning products appear at the surface.

Many observed features are well reproduced by current stellar models. Typically, good agreement is obtained between the observed and predicted values for the surface abundances of WN stars (Crowther et al 1995, Hamann & Koesterke 1998a). This indicates the general correctness of our understanding of the CNO cycle and of the relevant nuclear data (Maeder 1983), but is not a test of the model structure. For WC stars, comparisons with observed surface abundances also generally show good agreement (Willis 1991, Maeder & Meynet 1994). In particular, the strong surface Ne enrichments predicted by the models of WC stars have been confirmed by ISO observations (Willis et al 1997, 1998; Morris et al 1999; Dessart et al 1999).

The star number ratios W-R/O, W-R/RSG, and WN/WC show a strong correlation with metallicity (Azzopardi et al 1988, Smith 1988, Maeder 1991, Maeder & Meynet 1994, Massey & Johnson 1998). For instance, the W-R/O number ratio increases with the metallicity Z of the parent galaxy. Despite many other

claims (Bertelli & Chiosi 1981, 1982; Garmany et al 1982; Armandroff & Massey 1985; Massey 1985; Massey et al 1986), the main cause is metallicity Z, which through stellar winds influences stellar evolution and thus the W-R lifetimes (Smith 1973, Maeder et al 1980, Moffat & Shara 1983). The higher the metallicity, the stronger the mass loss by stellar winds, and thus the earlier the entry in the W-R phase for a given star; also, the minimum initial mass for forming a W-R star is lowered.

5.4.2 Remaining Problems with W-R Stars Despite the successes discussed previously, observations indicate some remaining problems:

1. It is possible to reproduce the W-R/O and WN/WC number ratios observed in the Milky Way and in various galaxies of the Local Group, but only by using models with mass loss rates enhanced by a factor of 2 during the MS and WNL phases (Maeder & Meynet 1994). The relative populations of WN and WC stars observed in young starburst regions are also better reproduced when models with high mass loss rates are used (Meynet 1995, Schaerer et al 1999). This is not satisfactory, because clumping in the winds of hot stars tends to reduce the observed mass loss rates by a factor of 2 to 3 (Nugis et al 1998; Hamann & Koesterke 1998b).
2. The lower limit for the luminosities of WN stars (around $\log L/L_{\odot} \sim 5.0$; Hamann & Koesterke 1998a) is fainter than that predicted by standard evolutionary tracks. Massey & Johnson (1998) found that the presence of luminous red supergiants (RSG) and W-R stars is well correlated for the OB associations in M31 and M33, which suggests that some stars with mass $\geq$15 $M_{\odot}$ go through both the RSG and W-R phases.
3. For WN stars, there is a continuous transition from high H-surface abundances (0.4–0.5 in mass fraction) to hydrogen-free atmospheres, whereas standard models predict an abrupt transition (Langer et al 1994, Hamann & Koesterke 1998a; see Figure 7 below).
4. Smith & Maeder (1998) showed that, besides the mass, a second parameter affecting the mass loss rates and terminal velocities of the wind is necessary to characterize the hydrogen-free WN stars.
5. Standard models do not reproduce the observed number of stars in the transition WN/WC phase, characterized by spectra with both H- and He-burning products. These models indeed predict an abrupt transition from WN to WC stars, because the He core is growing and thus building up a steep chemical discontinuity at its outer edge (e.g. Schaller et al 1992). Thus, almost no (<1%) stars with intermediate characteristics of WN and WC stars are predicted. However, 4–5% of the W-R stars are in such a transition phase (Conti & Massey 1989, van der Hucht 1999), which shows that some extra-mixing is at work (Langer 1991b).

5.4.3 Rotation and Formation of W-R Stars Rotation may affect the formation and properties of W-R stars in several ways (Sreenivasan & Wilson 1982, 1985a; Maeder 1987; Fliegner & Langer 1995; Maeder 1999b; Meynet 1999):

1. Surface abundances characteristic of the WNL stars may appear in a rotating star, not only as a result of the mass loss, which uncovers inner layers, but also as a result of mixing in radiative zones. The same remark applies to the entry into the WC phase.
2. Rotation may imply different evolutionary scenarios. Before becoming a W-R star, the nonrotating 60 $M_\odot$ model at solar metallicity is likely to go through a short LBV phase after the H exhaustion in its core. In the case of fast rotation, the star may enter the W-R phase while still burning hydrogen in its core (Maeder 1987, Fliegner & Langer 1995, Meynet 1999), thus skipping the LBV phase and spending more time in the W-R phase.
3. Rotation favors the formation of W-R stars from lower initial mass, through its effects on both the mass loss rates (Sreenivasan & Wilson 1982; Section 2.6) and the mixing. Typically, for the nonrotating models shown in Figure 5, the minimum mass for W-R star formation is between 35 and 40 $M_\odot$. It decreases to about 25 $M_\odot$ for initial $v_{\rm rot} = 300$ km/s. This effect may help to explain the low luminous WN stars reported by Hamann & Koesterke (1998a). It also favors entry into the W-R phase from the RSG stage.
4. During the WN phase, the surface abundances are different. Indeed, as a consequence of the first point in this list, the N/C, N/O ratios obtained at the surface of the rotating WN models may not yet have reached the full nuclear equilibrium, in contrast with the nonrotating case where nuclear equilibrium is reached as soon as the star enters the WN phase. However, the CNO ratios are close to the equilibrium values (see Figure 7). During the transition WN/WC phase, nitrogen enhancements can be observed simultaneously with carbon and neon enhancements. After this transition phase, the ^{22}Ne enhancement reaches more or less the same high equilibrium level regardless of the initial angular velocity, which agrees with determinations of the neon abundance at the surface of WC stars (Willis et al 1997).
5. Higher rotational velocities lead to longer W-R lifetimes. As an example, for a 60 $M_\odot$ model (Figure 7), the W-R lifetime is increased by more than a factor of 3 when rotation is included. The durations of the WN and of the transition WN/WC phases are increased. The ratio of the lifetimes of the WC to the WN phase is reduced.
6. High rotations lead to less luminous WC stars. This is because a rapidly rotating star enters the W-R stage earlier in its evolution and thus begins to lose large amounts of mass early. Therefore, fast rotators enter the WC phase with a small mass and a low luminosity; the final masses are also smaller.

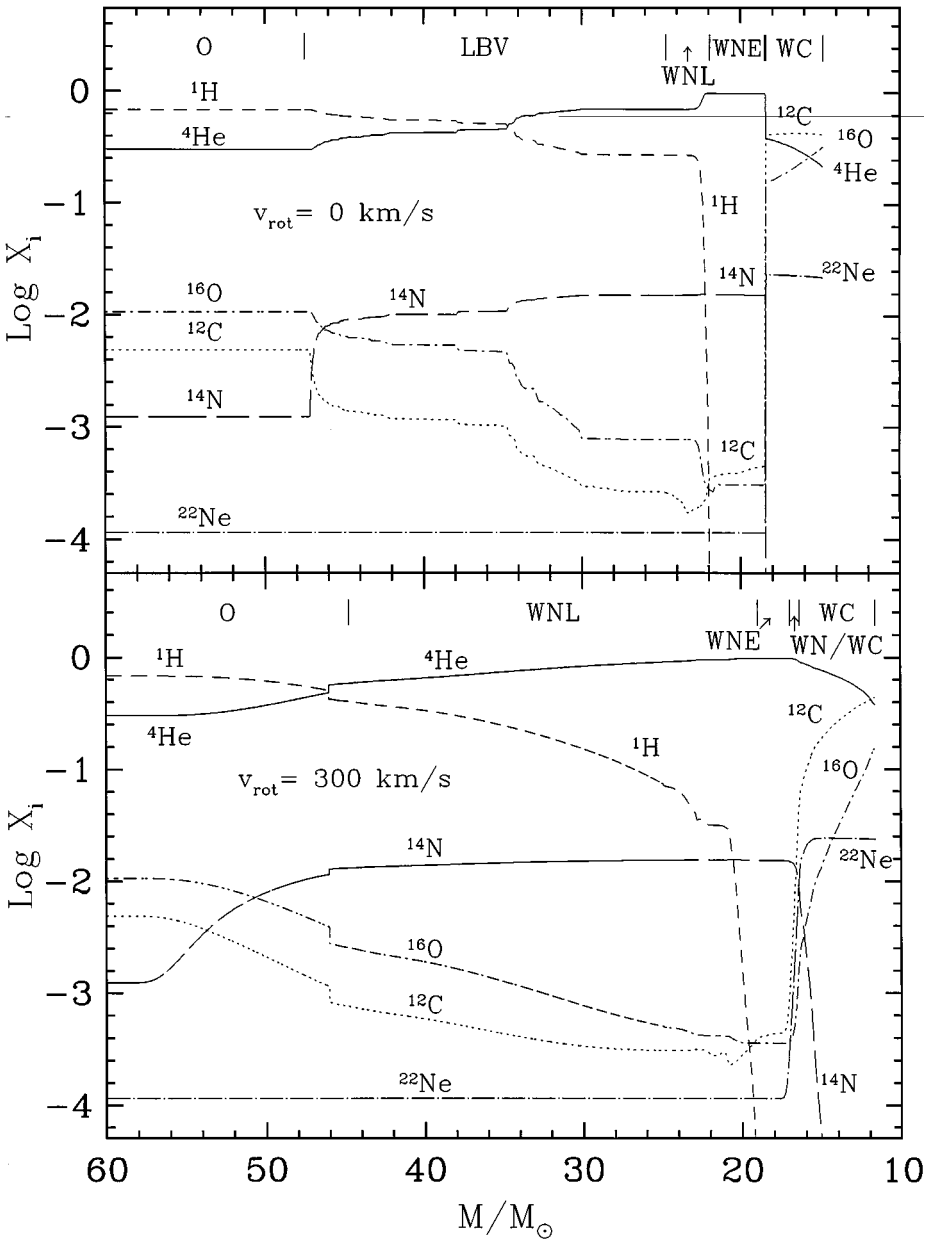

Figure 7 Evolution of the abundances at the surface of a 60 $M_\odot$ star as a function of the remaining stellar mass for different initial rotational velocities v_{rot}. The parts of the evolution during which the star may be considered as an O-type star, a LBV and a W–R star are indicated. During the W–R phase, the WN, the transition "WN/WC" and the WC phases are distinguished.

Rotation could thus remove or at least alleviate the problems mentioned above. The need to enhance the mass loss rates to reproduce the observed W-R/O number ratios no longer appears necessary. Rotation also implies effects that cannot be reproduced by an increase in the mass loss rate. In particular, mixing induced by rotation produces milder chemical gradients and leads to a more progressive decrease of the hydrogen abundance at the surface of WN stars (Figure 7).

5.4.4 Are W-R Stars Fast or Slow Rotators? Direct attempts to measure the rotational velocity of W-R stars have been performed only for a few cases. Massey (1980) and Koenigsberger (1990) obtained $v \sin i \sim 500$ km/s for WR138; however, the binary nature of this object (Annuk 1991) blurs this picture, because the origin of this high velocity might be the O-type companion. The second case, WR3 with $v \sin i \sim 150$–200 km/s, looks more promising (Massey & Conti 1981) because the broadened absorption lines move in phase with the W-R emission lines (Moffat et al 1986).

Indirect evidence points toward the existence of some axisymmetric features around W-R stars (see Drissen et al 1992, Marchenko 1994). For instance, Arnal (1992) has mapped the environment of six W-R stars at a frequency of 1.42 MHz and found that all the HI cavities around these have an elongated shape with a mean major-to-minor axis ratio of about 2.2. Other evidence of anisotropies was found by Schulte-Ladbeck et al (1992) and Miller & Chu (1993). According to Harries et al (1998), about 15% of W-R stars have anisotropic winds. They suggest that the main cause of the wind anisotropy is equatorial density enhancements produced by fast rotation rates, and estimate the rotational velocities to be about 10–20% of the breakup velocity.

The surface velocities of W-R stars depend mainly on the initial velocity and on the amount of angular momentum lost during the previous stages. This amount will depend on the exact evolutionary sequence followed; in particular, the questions are whether the star has passed through the RSG stage and what were the anisotropies of the stellar winds. Some other effects may also intervene, for instance the possible presence of a magnetic field (e.g. Cassinelli 1992, Sreenivasan & Wilson 1982; Section 3.2).

For the 60 $M_\odot$ model shown in Figure 7 with $v_{\rm rot} = 300$ km/s, computed assuming spherically symmetric winds and no magnetic fields, the surface velocity ranges between 20 and 40 km/s, i.e. between 3% and 6% of the breakup velocity during most of the WNL phase. At the beginning of the core He-burning phase, the He core contracts, the small H-rich envelope expands, and the surface velocity reaches the breakup limit. Huge mass loss rates ensue, ejecting about 3 $M_\odot$ of material and forming an anisotropic nebula with abundances characteristic of CNO equilibrium. When the star has lost sufficient angular momentum, it drops below the breakup limit and pursues its evolution with a nearly constant surface velocity around 40 km/s. The contraction of the W-R star at the very end of the He-burning phase may again increase $v_{\rm rot}$, but it remains far below the breakup limit ($\Omega/\Omega_{\rm crit} \sim 5\%$).

5.5 Late Stages, Remnants, and Chemical Yields

5.5.1 The Post–He-Burning Phases The masses of the C/O cores are larger in rotating stars, which do not evolve through a W-R phase (Sofia et al 1994, Heger et al 2000). For example, at the end of the He-burning phase, the C/O core mass in a rotating 20 $M_\odot$ model with an initial $v_{rot} = 300$ km/s is 5.7 $M_\odot$ (Meynet & Maeder 2000). The value in a nonrotating model is 3.8 $M_\odot$. Thus, a rotating 20 $M_\odot$ star will have a behavior during the late stages similar to that of a nonrotating 25 $M_\odot$ star.

It is also interesting to notice that because of the larger He cores, the $^{12}C(\alpha,\gamma)^{16}O$ reaction is more active at the end of the He-burning phase; therefore, the fraction of carbon left in the C/O core decreases with respect to that in the nonrotating model (by a factor of about 2.5 in the preceding example). This leads to an increase in the oxygen yield. Moreover, since the carbon burning phase is considerably reduced, the stellar core has less time to remove its entropy through heavy neutrino losses, thus favoring the formation of black holes (Woosley 1986). According to Fryer (1999) the lower mass limit for black hole formation is likely lowered by rotation (see also Fryer & Heger 1999).

After central He exhaustion, the He-shell ignites and the layers above it expand, leading to a decrease in the strength of the H-burning shell. The smaller thermal gradient near the H-shell favors the mixing of chemical elements there (Heger et al 2000). Protons are brought from the H-shell down into the underlying He-rich layers where they will be engulfed by the convective He-burning shell. At the same time, because of the contraction of the C/O core, the temperature at the bottom of the He-shell increases and the overlying convective zone extends in mass, engulfing the region that is rotationally enriched in protons and nitrogen. These species then burn very rapidly, on a timescale shorter than the convective turnover time; thus, they have almost completely disappeared before reaching the bottom of the He-convective zone (Heger 1998). The large extension of the He-burning shell has important consequences for nucleosynthesis. This extension is greater for larger core masses, i.e. for large initial mass and/or for large rotational velocities.

When evolution proceeds further, the rotating core speeds up more and more, possibly becoming unstable with respect to nonaxisymmetric perturbations (Kippenhahn et al 1970, Ostriker & Bodenheimer 1973, Tassoul 1978). However, the results obtained by Heger et al (2000) for stars with initial v_{rot} between 200 and 300 km/s suggest that, before the core collapse, the ratio of rotational to potential energy is lower than that required for such instabilities to occur.

5.5.2 Rotational Periods of Pulsars According to the models by Heger et al (2000), at their birth neutron stars (NS) should have rotation periods of about 0.6 ms, since they are nearly at the breakup rate. What is striking is that these periods are much smaller than the measured periods for young pulsars, which are around 20–150 ms (Marshall et al 1998). This means that the models have

between ∼20 and 100 times more specific angular momentum than is found in the young neutron stars. Various effects may be responsible for this excess rotation in the models. The efficiency of some rotationally induced mixing processes may have been underestimated, or some important transport mechanism may still be missing. Kippenhahn et al (1970) speculated about the possibility for rapidly rotating dense cores to shed some mass into the envelope at its equator, in a way similar to rapidly rotating stars shedding mass into the circumstellar envelope. The equatorial mass loss by anisotropic stellar winds heavily modifies the surface boundary conditions and may remove a huge amount of angular momentum (Maeder 1999a). Other braking mechanisms, such as the removal of angular momentum from the convective core by gravity waves (Denissenkov et al 1999; Section 2.5) or through a magnetic field (Spruit & Phinney 1998), may also be invoked. As pointed out by Fricke & Kippenhahn (1972), the coupling of the core and envelope cannot be complete because, with solid body rotation at all times, the core would rotate too slowly ($P \simeq 650$ ms) to form pulsars with the observed periods.

The evacuation of the excess angular momentum could also have occurred during the formation of a neutron star. The NS could also have been born spinning at breakup velocity and could have been very efficiently slowed down during the first years. However, as discussed by Hardorp (1974), some arguments suggest that NS have never been near breakup (Rudermann 1972); the study of the Crab pulsar supports this view (Trimble & Rees 1970). Indeed, in this case, the release of such an important amount of rotational energy, if not emitted in the form of a γ-ray burst or through gravitational waves, would have shown up in the expansion energy of the nebula and in the optical light during historical times, which was not reported. The original rotation period of the Crab pulsar at birth is estimated to be 5 ms, still one order of magnitude from the breakup period (Hardorp 1974). Therefore, the stellar core must have been spinning slowly before its collapse.

If a large angular momentum is embarrassing at present when we explain the observed rotating periods of young pulsars, it may give some support to the collapsar model proposed by Woosley (1993; MacFadyen & Woosley 1999) for the γ-ray bursts. A collapsar is a black hole formed by the incomplete explosion of a rapidly rotating massive star. The rapid rotation is necessary to allow the formation of an accretion disk outside the black hole. The accretion disk efficiently transforms the gravitational binding energy into heat which can then power a highly relativistic jet. The burst and its afterglow in various wavelengths are attributed to the jet and its interactions with the external medium. The models by Heger et al (2000) and Meynet & Maeder (2000) have enough angular momentum to support matter in a stable disk outside a black hole, and thus could offer interesting progenitors for this kind of evolution, if it exists.

5.5.3 Chemical Yields Rotation affects chemical yields in many ways. The larger He cores obtained in rotating models at core collapse imply larger production

of helium and other α-nuclei elements (Heger 1998). This is by far the most important effect of rotation on chemical yields. Also, by enhancing the mass loss rates and by making the formation of W-R stars easier, rotation favors the enrichment of the interstellar medium by stellar winds (Maeder 1992). Indeed, the stronger the winds, the richer the ejecta in helium and carbon and the lower the ejecta in oxygen.

The rotational diffusion during the H-burning phase enriches the outer layers in CNO-processed elements (Maeder 1987, Fliegner & Langer 1995, Meynet 1998, Heger 1998). Some ^{14}N is extracted from the core and saved from further destruction. The same can be said for ^{17}O and ^{26}Al, a radioisotope with a half-life of 0.72 M. The mixing in the envelope of rotating stars also leads to faster depletion of the temperature-sensitive light isotopes, for instance lithium and boron (Fliegner et al 1996).

The presence of ^{26}Al in the interstellar medium is responsible for the diffuse galactic emission observed at 1.8 MeV (e.g. Oberlack et al 1996). If the nucleosynthetic sites of this element appear to be the massive stars (Prantzos & Diehl 1996), it is still not clear how the production is shared between the supernovae and the W-R stars, and how it is affected by rotation and binarity. For stellar masses between 12 and 15 $M_\odot$, the lifetimes are much longer than that of ^{26}Al, and therefore most of the ^{26}Al produced during central H-burning and partially mixed in the envelope has decayed at the time of the supernova explosion. Thus, for this mass range, rotation does not seem to effect important changes (Heger 1998). However, when the star is massive enough to go through the W-R phase, the stellar winds may remove ^{26}Al-enriched layers at a much earlier stage. In this case, rotation may substantially increase the quantity of ^{26}Al injected in the interstellar medium (Langer et al 1995).

The convective zone associated with the He-shell in rotating models transports H-burning products to the He-burning shell (Heger 1998). The injection of protons and nitrogen into a He-burning zone opens new channels of nucleosynthesis (Jorissen & Arnould 1989). In particular, this enhances the s-process and the formation of ^{14}C, ^{18}O, and ^{19}F. Because these elements are produced just before the core collapse, they can survive until the supernova explosion. The injection of protons into a He-burning zone may also be responsible for primary ^{14}N production through ^{12}C(p,γ)^{13}N(β^+)^{13}C(p,γ)^{14}N, but this primary nitrogen is rapidly destroyed to produce ^{18}O. As we discussed in Section 4.2, stars with an He-burning core and a thick and long-lived H-burning shell seem to be more favorable sites for primary ^{14}N production. Another important effect of the growth of the He-shell in these late stages is the production of some ^{15}N shortly before core collapse. In nonrotating models this element is destroyed, whereas in rotating models it is synthesized (Heger 1998). The very low ^{14}N/^{15}N ratios measured in star-forming regions of the LMC and in the core of the (post-) starburst galaxy NGC 4945 (Chin et al 1999) support an origin of ^{15}N in massive stars.

6. PERSPECTIVES

We hope to have shown that rotation is indispensable for a proper understanding and modeling of the evolution for the Upper MS stars.

Further progress requires more studies of the physical effects of rotation, in particular of the various instabilities that can produce mixing of the elements and transport of angular momentum, both in the early and advanced phases of evolution. The influence of rotation on mass loss is also critical. In this respect, the shape and composition of the asymmetric nebulae observed around many massive stars provide interesting constraints on the models of rotating stars.

ACKNOWLEDGMENTS

We express our thanks to Dr. Laura Fullton for her most useful advice on the manuscript.

LITERATURE CITED

Abbott DC, Conti PS. 1987. *Annu. Rev. Astron. Astrophys.* 25:113–50

Annuk K. 1991. In *Wolf-Rayet Stars and Interrelations with Other Massive Stars in Galaxies*, IAU Symp. 143, ed. KA van der Hucht, B Hidayat, pp. 245–50. Dordrecht: Kluwer

Armandroff TE, Massey P. 1985. *Ap. J.* 291:685–92

Arnal EM. 1992. *Astron. Astrophys.* 250:171–78

Arnett D. 1991. *Ap. J.* 383:295–307

Azzopardi M, Lequeux J, Maeder A. 1988. *Astron. Astrophys.* 189:34–38

Barbuy B, De Medeiros JR, Maeder A. 1996. *Astron. Astrophys.* 305:911–19

Bertelli G, Chiosi C. 1981. In *The Most Massive Stars*, ed. S d'Odorico, D Baade, K Kjär, pp. 211–13. ESO Workshop, ESO Publ, Garchingb. München

Bertelli G, Chiosi C. 1982. In *Wolf–Rayet Stars: Observations, Physics, Evolution*, IAU Symp. 99, ed. CWH de Loore, AJ Willis, pp. 359–63. Dordrecht: Reidel

Bjorkman JE, Cassinelli JP. 1993. *Ap. J.* 409:429–49

Bodenheimer P. 1995. *Annu. Rev. Astron. Astrophys.* 33:199–238

Boothroyd AI, Sackmann IJ. 1999. *Ap. J.* 510: 232–50

Boyarchuk AA, Lyubimkov LS. 1983. *Izv. Krym. Astrofiz. Obs.* 66:130

Bressan A, Fagotto F, Bertelli G, Chiosi C. 1993. *Astron. Astrophys.* 100:647–64

Brocato E, Castellani V. 1993. *Ap. J.* 410:99–109

Brunish WM, Gallagher JS, Truran JW. 1986. *Astron. J.* 91:598–601

Burrows CJ, Krist J, Hester JJ, Sahai R, Trauger JT, et al. 1995. *Ap. J.* 452:680–84

Canuto VM. 1994. *Ap. J.* 428:729–52

Canuto VM. 1998. *Ap. J.* 508:767–79

Canuto VM, Dubovikov M. 1997. *Ap. J. Lett.* 484:161–63

Canuto VM, Goldman I, Mazzitelli I. 1996. *Ap. J.* 473:550–59

Canuto VM, Minotti FO, Schilling O. 1994. *Ap. J.* 425:303–25

Cassinelli JP. 1992. See Drissen et al 1992, pp. 134–44

Centurion M, Bonifacio P, Molaro P, Vladilo G. 1998. *Ap. J.* 509:620–32

Cervino M, Mas-Hesse JM. 1994. *Astron. Astrophys.* 284:749–63

Chaboyer B, Demarque P, Pinsonneault MH. 1995a. *Ap. J.* 441:865–75

Chaboyer B, Demarque P, Pinsonneault MH. 1995b. *Ap. J.* 441:876–85

Chaboyer B, Zahn JP. 1992. *Astron. Astrophys.* 253:173–77

Chandrasekhar S. 1961. In *Hydrodynamic and Hydromagnetic Stability*, Oxford: Clarendon Press, p. 491

Charbonnel C. 1994. *Astron. Astrophys.* 282:811–20

Charbonnel C, Brown JA, Wallerstein G. 1998. *Astron. Astrophys.* 332:204–14

Chin CW, Stothers RB. 1991. *Ap. J. Suppl.* 77:299–316

Chin Y, Henkel C, Langer N, Mauersberger R. 1999. *Ap. J.* 512:L143–46

Chiosi C, Maeder A. 1986. *Annu. Rev. Astron. Astrophys.* 24:329–75

Chiosi C, Nasi E, Sreenivasan SR. 1978. *Astron. Astrophys.* 63:103–24

Collins GW, Sonneborn GH. 1977. *Ap. J. Suppl.* 34:41–94

Conti PS. 1984. In *Observational Tests of the Stellar Evolution Theory*, IAU Symp. 105, ed. A Maeder, A Renzini, pp. 233–54. Dordrecht: Reidel

Conti PS, Ebbets D. 1977. *Ap. J.* 213:438–47

Conti PS, Garmany CD, de Loore C, Vanbeveren D. 1983. *Ap. J.* 274:302–12

Conti PS, Massey P. 1989. *Ap. J.* 337:251–71

Cowley AP, Dawson P, Hartwick FDA. 1979. *Publ. Astron. Soc. Pac.* 91:628–31

Cox JP, Giuli RT. 1968. *Stellar Structure.* New York: Gordon & Breach. p. 307

Crowther PA. 1997. See Wolf et al 1999, pp. 51–57

Crowther PA, Hillier DJ, Smith LJ. 1995. *Astron. Astrophys.* 293:403–26

Damineli A. 1996. *Ap. J. Lett.* 460:49–52

Damineli A, Conti PS, Lopes DF. 1997. *New Astron.* 2:107–17

Davidson K, Dufour RJ, Walborn NR, Gull TR. 1986. *Ap. J.* 305:867–79

Davidson K, Ebbets D, Johansson S, Morse JA, Hamann FW. 1997. *Astron. J.* 113:335–45

Davidson K, Humphreys RM. 1997. *Annu. Rev. Astron. Astrophys.* 35:1–32

Davidson K, Moffat AFJ, Lamers HJGLM. 1989. In *Physics of Luminous Blue Variables*, IAU Coll. 113, ed. A. Nota, HJGLM Lamers, Dordrecht: Kluwer. 404 pp.

Dearborn DSP. 1992. *Phys. Rep.* 210:367

de Jager C, Nieuwenhuijzen H. 1992. In *Instabilities in Evolved Super- and Hypergiants*, ed. C. de Jager, H. Nieuwenhuijzen. Amsterdam: North-Holland. 199 pp.

de Jager C, Nieuwenhuijzen H, van der Hucht KA. 1988. *Astron. Astrophys. Suppl.* 72:259–89

Denissenkov PA. 1994. *Astron. Astrophys.* 287:113–30

Denissenkov PA, Ivanova NS, Weiss A. 1999. *Astron. Astrophys.* 341:181–89

Dessart L, Willis AJ, Crowther PA, Morris PW, Hillier DJ. 1999. See van der Hucht et al 1999, pp. 233–34

Deupree RG. 1995. *Ap. J.* 439:357–64

Deupree RG. 1998. *Ap. J.* 499:340–47

Dominguez I, Straniero O, Tornambé A. 1996. *Ap. J.* 472:783–88

Drissen L, Leitherer C, Nota A. 1992. *Non-isotropic and Variable Outflows from Stars, ASP Conf. Ser.* San Francisco: Astron. Soc. Pacific 22:408

Dwarkadas VV, Balick B. 1998. *Astron. J.* 116:829–39

Eddington AS. 1925. *The Observatory* 48:73–75

Edmunds MG, Pagel BEJ. 1978. *MNRAS* 185:77–80

El Eid MF. 1994. *Astron. Astrophys.* 285:915–28

Endal AS, Sofia S. 1976. *Ap. J.* 210:184–98

Endal AS, Sofia S. 1978. *Ap. J.* 220:279–90

Endal AS, Sofia S. 1979. *Ap. J.* 232:531–40

Eriguchi Y, Yamaoka H, Nomoto K, Hashimoto M. 1992. *Ap. J.* 392:243–48

Eryurt D, Kirbiyik H, Kiziloglu N, Civelek R,

Weiss A. 1994. *Astron. Astrophys.* 282:485–92

Fagotto F, Bressan A, Bertelli G, Chiosi C. 1994. *Astron. Astrophys. Suppl. Ser.* 105:39–45

Faulkner J, Roxburgh IW, Strittmatter PA. 1968. *Ap. J.* 151:203–16

Fliegner J, Langer N. 1995. In *Wolf-Rayet Stars: Binaries, Colliding Winds, Evolution*, IAU Symp. 163, ed. KA van der Hucht, PM Williams, pp. 326–28. Dordrecht: Kluwer

Fliegner J, Langer N, Venn KA. 1996. *Astron. Astrophys.* 308:L13–16

Frank A, Balick B, Davidson K. 1995. *Ap. J.* 441:L77–80

Frank A, Ryu D, Davidson K. 1998. *Ap. J.* 500:291–301

Fransson C, Cassatella A, Gilmozzi R, Kirshner RP, Panagia N, Sonneborn G, Wamsteker W. 1989. *Ap. J.* 336:429–41

Fricke KJ. 1968. *Zeitschr. Ap.* 68:317–44

Fricke KJ, Kippenhahn R. 1972. *Annu. Rev. Astron. Astrophys.* 10:45–72

Friend DB, Abbott DC. 1986. *Ap. J.* 311:701–7

Fryer CL. 1999. *Ap. J.* 522:413–18

Fryer CL, Heger A. 1999. astro-ph /9907433

Fukuda I. 1982. *Publ. Astron. Soc. Pac.* 92:271–84

Garcia-Segura G, Langer N, Mac Low MM. 1997. See Nota & Lamers 1997, pp. 121–27.

Garcia-Segura G, Langer N, Rózyczka M, Franco J. 1999. *Ap. J.* 517:767–81

Garcia–Segura G, Mac Low MM, Langer N. 1996. *Astron. Astrophys.* 305:229–44

Garmany CD, Conti PS, Chiosi C. 1982. *Ap. J.* 263:777–90

Giannone P, Kohl K, Weigert A. 1968. *Z. Astrophys.* 68:107–29

Gies DR, Lambert DL. 1992. *Ap. J.* 387:673–700

Gilroy KK. 1989. *Ap. J.* 347:835–48

Gilroy KK, Brown JA. 1991. *Ap. J.* 371:578–83

Glatzel W. 1998. *Astron. Astrophys.* 339:L5–8

Glatzel W, Kiriakidis M. 1998. *MNRAS* 295:251–56

Goldreich P, Schubert G. 1967. *Ap. J.* 150:571–87

Groenewegen MAT, Lamers HJGLM, Pauldrach A. 1989. *Astron. Astrophys.* 221:78–88

Guilloteau S, Dutrey A. 1998. *Astron. Astrophys.* 339:467–76

Hamann WR, Koesterke L. 1998a. *Astron. Astrophys.* 333:251–63

Hamann WR, Koesterke L. 1998b. *Astron. Astrophys.* 335:1003–8

Hamann WR, Koesterke L, Wessolowski U. 1993. *Astron. Astrophys.* 274:397–414

Hardorp J. 1974. *Astron. Astrophys.* 32:133–36

Harries TJ, Hillier DJ, Howarth ID. 1998. *MNRAS* 296:1072–88

Harris MJ, Lambert DL, Smith VV. 1988. *Ap. J.* 325:768–75

Hartmann LW, Noyes RW. 1987. *Annu. Rev. Astron. Astrophys.* 25:271–01

Heger A. 1998. PhD thesis. Max-Planck-Institut für Astrophysik. *MPA* 1120

Heger A, Langer N. 1998. *Astron. Astrophys.* 334:210–20

Heger A, Langer N, Woosley SE. 2000. *Ap. J.* 528:368–396

Henry RBC, Worthey G. 1999. *Publ. Astron. Soc. Pac.* 111:919–45

Herrero A, Corral LJ, Villamariz MR, Martin EL. 1999. *Astron. Astrophys.* 348:542–52

Herrero A, Kudritzki RP, Vilchez JM, Kunze D, Butler K, Haser S. 1992. *Astron. Astrophys.* 261:209–34

Herrero A, Villamariz MR, Martin EL. 1998. See Howarth 1998, pp. 159–68

Howarth ID. 1998. *Boulder–Munich II: Properties of Hot, Luminous Stars*, ASP Conf. Ser. San Francisco, 131:456. Astron. Soc. Pacific

Howarth ID, Siebert KW, Hussain GAJ, Prinja RK. 1997. *MNRAS* 284:265–85

Humphreys RM. 1989. In *Physics of Luminous Blue Variables*, ed. K Davidson, AFJ Moffat, HJGLM Lamers, pp 1–14. Dordrecht: Kluwer

Humphreys RM, McElroy DB. 1984. *Ap. J.* 284:565–77

Humphreys RM, Nichols M, Massey P. 1985. *Astron. J.* 90:101–8

Iben I. 1999. See Le Bertre et al 1999, p. 591

Jeans JH. 1928. In *Astronomy and Cosmogony*, p. 273. Cambridge, UK: Cambridge Univ. Press

Jorissen A, Arnould M. 1989. *Astron. Astrophys.* 221:161–79

Kato S. 1966. *Publ. Astron. Soc. Pac.* 18:374–83

Kendall TR, Dufton PL, Lennon DJ. 1996. *Astron. Astrophys.* 310:564–76

Kendall TR, Lennon DJ, Brown PJF, Dufton PL. 1995. *Astron. Astrophys.* 298:489–504

Kilian J. 1992. *Astron. Astrophys.* 262:171–87

Kippenhahn R. 1974. In *Late Stages of Stellar Evolution*, IAU Symp. 66, ed. RJ Tayler, JE Hesser, pp. 20–40. Dordrecht: Reidel

Kippenhahn R. 1977. *Astron. Astrophys.* 58:267–71

Kippenhahn R, Meyer-Hofmeister E, Thomas HC. 1970. *Astron. Astrophys.* 5:155–61

Kippenhahn R, Thomas HC. 1970. See Slettebak 1970, pp. 20–29

Kippenhahn R, Weigert A. 1990. In *Stellar Structure and Evolution.* Berlin: Springer Verlag. 468 pp.

Knobloch E, Spruit HC. 1983. *Astron. Astrophys.* 125:59–68

Koenigsberger G. 1990. *Rev. Mex. Astron. Astrofis.* 20:85–112

Korycansky DG. 1991. *Ap. J.* 381:515–25

Kraft RP. 1966. *Ap. J.* 144:1008–15

Kraft RP, Camp DC, Fernie JD, Fujita C, Hughes WT. 1959. *Ap. J.* 129:50–8

Kudritzki RP, Hummer DG, Pauldrach A, Puls J, Najarro F, Imhoff J. 1992. *Astron. Astrophys.* 257:655–62

Kudritzki RP, Pauldrach A, Puls J, Abbott DC. 1989. *Astron. Astrophys.* 219:205–18

Kumar P, Narayan R, Loeb A. 1995. *Ap. J.* 453:480–94

Kumar P, Quataert EJ. 1997. *Ap. J. Lett.* 475:43–46

Lamers HJGLM. 1997. See Nota & Lamers 1997, pp. 79–82.

Lamers HJGLM. 1999. See Wolf et al 1999, pp. 159–68

Lamers HJGLM, Cassinelli JP. 1996. See Leitherer et al 1996, pp. 162–73

Lamers, HJGLM, Leitherer C. 1993. *Ap. J.* 412:471–91

Lamers HJGLM, Maeder A, Schmutz W, Cassinelli JP. 1991. *Ap. J.* 368:538–44

Langer N. 1991a. *Astron. Astrophys.* 243:155–59

Langer N. 1991b. *Astron. Astrophys.* 248:531–37

Langer N. 1991c. *Astron. Astrophys.* 252:669–88

Langer N. 1992. *Astron. Astrophys.* 265:L17–20

Langer N. 1997. See Nota & Lamers 1997, pp. 83–89

Langer N. 1998. *Astron. Astrophys.* 329:551–58

Langer N. 1999. See Wolf et al 1999, pp. 359–67

Langer N, Braun H, Fliegner J. 1995. *Astrophys. Space Sci.* 224:275–78

Langer N, Fricke KJ, Sugimoto D. 1983. *Astron. Astrophys.* 126:207–8

Langer N, Garcia-Segura G, Mac Low MM. 1999a. *Ap. J. Lett.* 520:49–53

Langer N, Hamann WR, Lennon M, Najarro F, Pauldrach AWA, Puls J. 1994. *Astron. Astrophys.* 290:819–33

Langer N, Heger A. 1998. See Howarth 1998, pp. 76–84

Langer N, Heger A, Wellstein S, Herwig F. 1999b. *Astron. Astrophys.* 346:L37–40

Langer N, Maeder A. 1995. *Astron. Astrophys.* 295:685–92

Lanz T, de Koter A, Hubeny I, Heap SR. 1996. *Ap. J.* 465:359–62

Le Bertre T, Lèbre A, Waelkens C. 1999. *Asymptotic Giant Branch Stars, IAU Symp. 191, Publ. Astron. Soc. Pac* 632 pp.

Ledoux P. 1958. Stellar Stability, in *Handbuch der Physik, 51: Astrophysik II: Sternaufbau.*,

ed. S. Flügge. pp. 605–688. Berlin: Springer Verlag. 830 pp.

Leitherer C, Fritze-von Alvensleben U, Huchra T. 1996. *From Stars to Galaxies: The Impact of Stellar Physics on Galaxy Evolution, ASP Conf. Ser. 98,* pp. 624: Astron. Soc Pacific, San Francisco

Lennon DJ, Becker ST, Butler K, Eber F, Groth HG, et al. 1991. *Astron. Astrophys.* 252:498–507

Lloyd HM, O'Brien TJ, Kahn FD. 1995. *MNRAS* 273:L19–23

Luck RE. 1978. *Ap. J.* 219:148–64

Lundqvist P, Fransson C. 1996. *Ap. J.* 464:924–42

Lyubimkov LS. 1991. See Michaud & Tutukov 1991, pp. 125–35

Lyubimkov LS. 1996. *Astroph. Space Sci.* 243:329–49

Lyubimkov LS. 1998. *Astron. Rep.* 42:53–9

MacFadyen AI, Woosley SE. 1999. *Ap. J.* 524:262–289

MacGregor KB, Friend DB, Gilliland RL. 1992. *Astron. Astrophys.* 256:141–47

Maeder A. 1971. *Astron. Astrophys.* 10:354–61

Maeder A. 1974. *Astron. Astrophys.* 34:409–14

Maeder A. 1981. *Astron. Astrophys.* 102:401–10

Maeder A. 1983. *Astron. Astrophys.* 120:113–35

Maeder A. 1987. *Astron. Astrophys.* 178:159–69

Maeder A. 1991. *Astron. Astrophys.* 242:93–111

Maeder A. 1992. *Astron. Astrophys.* 264:105–20

Maeder A. 1995. *Astron. Astrophys.* 299:84–88

Maeder A. 1997. *Astron. Astrophys.* 321:134–44

Maeder A. 1998. See Howarth 1998, pp. 85–95

Maeder A. 1999a. *Astron. Astrophys.* 347:185–93

Maeder A. 1999b. See van der Hucht et al 1999, pp. 177–86

Maeder A, Conti P. 1994. *Annu. Rev. Astron. Astrophys.* 32:227–75

Maeder A, Grebel E, Mermilliod JC. 1999. *Astron. Astrophys.* 346:459–64

Maeder A, Lequeux J, Azzopardi M. 1980. *Astron. Astrophys.* 90:L17–20

Maeder A, Meynet G. 1989. *Astron. Astrophys.* 210:155–73

Maeder A, Meynet G. 1994. *Astron. Astrophys.* 287:803–16

Maeder A, Meynet G. 1996. *Astron. Astrophys.* 313:140–44

Maeder A, Peytremann E. 1970. *Astron. Astrophys.* 7:120–32

Maeder A, Zahn JP. 1998. *Astron. Astrophys.* 334:1000–6

Marchenko SV. 1994. *Astrophys. Space Sci.* 221:169–80

Marshall FE, Gotthelf EV, Zhang W, Middleditch J, Wang QD. 1998. *Ap. J.* 499:L179–82

Marston AP. 1997. *Ap. J.* 475:188–93

Martin CL, Arnett D. 1995. *Ap. J.* 447:378–90

Massey P. 1980. *Ap. J.* 236:526–35

Massey P. 1985. *Publ. Astron. Soc. Pac.* 97:5–24

Massey P, Armandroff TE, Conti PS. 1986. *Astron. J.* 92:1303–33

Massey P, Conti PS. 1981. *Ap. J.* 244:173–78

Massey P, Johnson O. 1998. *Ap. J.* 505:793–827

Mathys G. 1999. See Wolf et al 1999, pp. 95–102

Matteucci F. 1986. *MNRAS* 221:911–21

McEarlean ND. 1998. See Howarth 1998, pp. 148–52

McEarlean ND, Lennon DJ, Dufton PL. 1999. *Astron. Astrophys.* 349:553–72

Meaburn J, Bryce M, Holloway AJ. 1995. *Astron. Astrophys.* 299:L1–4

Mestel L. 1953. *MNRAS* 113:716–45

Mestel L. 1965. In *Stellar Structure*, ed. LH Aller, DB McLaughlin, pp. 465–97. Chicago: Univ. Chicago Press

Meylan G, Maeder A. 1982. *Astron. Astrophys.* 108:148–56

Meynet G. 1995. *Astron. Astrophys.* 298:767–83
Meynet G. 1998. See Howarth 1998, pp. 96–107
Meynet G. 1999. See Wolf et al 1999, pp. 377–80
Meynet G. 2000. In *Spectrophotometric Dating of Stars and Galaxies,*ASP Conf. Ser., ed. I Hubeny, S Heap, R Cornett. In press
Meynet G, Maeder A. 1997. *Astron. Astrophys.* 321:465–76
Meynet G, Maeder A. 2000. *Astron. Astrophys.* In press
Michaud G, Tutukov AV. 1991. *Evolution of Stars: The Photospheric Abundance Connection, IAU Symp. 145*, Dordrecht: Kluwer Acad. Publ., pp. 487
Miller GJ, Chu YH. 1993. *Ap. J. Suppl.* 85:137–43
Milne EA. 1923. *MNRAS* 83:118– 47
Moffat AFJ, Lamontagne R, Shara MM, McAlister HA. 1986. *Astron. J.* 91:1392–99
Moffat AFJ, Shara MM. 1983. *Ap. J.* 273:544 – 61
Montalban J. 1994. *Astron. Astrophys.* 281:421–32
Montalban J, Schatzman E. 1996. *Astron. Astrophys.* 305:513–18
Morris PW, van der Hucht KA, Willis AJ, Dessart L, Crowther PA, Williams PM. 1999. See van der Hucht et al 1999, pp. 77–79
Nieuwenhuijzen H, de Jager C. 1988. *Astron. Astrophys.* 203:355–60
Nota A, Clampin M. 1997. See Nota & Lamers 1997, pp. 303–9
Nota A, Lamers HJGLM. 1997. *Luminous Blue Variables: Massive Stars in Transition.* ASP Conf. Ser. 120. San Francisco: Astron. Soc. of Pacific, 404 pp.
Nota A, Livio M, Clampin M, Schulte-Ladbeck R. 1995. *Ap. J.* 448:788–96
Nota A, Smith L, Pasquali A, Clampin M, Stroud M. 1997. *Ap. J.* 486:338–54
Nugis T, Crowther PA, Willis AJ. 1998. *Astron. Astrophys.* 333:956–69
Oberlack U, Bennett K, Bloemen H, Diehl R, Dupraz C, et al. 1996. *Astron. Astrophys. Suppl.* 120:311–14
Oke JB, Greenstein JL. 1954. *Ap. J.* 120:384 – 90
Origlia L, Goldader JD, Leitherer C, Schaerer D, Oliva E. 1999. *Ap. J.* 514:96–108
Ostriker JP, Bodenheimer P. 1973. *Ap. J.* 180:171–80
Owocki SP, Cranmer SR, Gayley KG. 1996. *Ap. J. Lett.* 472:115–18
Owocki SP, Gayley KG. 1997. See Nota & Lamers 1997, pp. 121–27
Owocki SP, Gayley KG. 1998. See Howarth 1998, pp. 237– 44
Packet W, Vanbeveren D, De Greve JP, de Loore C, Sreenivasan R. 1980. *Astron. Astrophys.* 82:73–78
Panagia N, Scuderi S, Gilmozzi R, Challis PM, Garnavich PM, Kirshner RP. 1996. *Ap. J.* 459:L17–21
Pauldrach A, Puls J, Kudritzki RP. 1986. *Astron. Astrophys.* 164:86–100
Penny LR. 1996. *Ap. J.* 463:737– 46
Penny LR, Gies DR, Bagnuolo WG. 1999. See van der Hucht et al 1999, pp. 86–89
Pettini M, Lipman K, Hunstead RW. 1995. *Ap. J.* 451:100–10
Pilyugin LS. 1999. *Astron. Astrophys.* 346: 428–31
Pinsonneault M. 1997. *Annu. Rev. Astron. Astrophys.* 35:557–605
Pinsonneault MH, Delyannis CP, Demarque P. 1991. *Ap. J.* 367:239–52
Pinsonneault MH, Kawaler SD, Demarque P. 1990. *Ap. J. Suppl.* 74:501–50
Pinsonneault MH, Kawaler SD, Sofia S, Demarque P. 1989. *Ap. J. Suppl.* 338:424 – 52
Poe CH, Friend DB. 1986. *Ap. J.* 311:317–25
Prantzos N, Coc A, Thibaud JP. 1991. *Ap. J.* 379:729–33
Prantzos N, Diehl R. 1996. *Phys. Rep.* 267:1–69
Randers G. 1941. *Ap. J.* 94:109–23
Ringot O. 1998. *Astron. Astrophys.* 335:L89–92
Rosendhal JD. 1970. *Ap. J.* 159:107–18

Rudermann M. 1972. *Annu. Rev. Astron. Astrophys.* 10:427–76
Sackmann IJ, Anand SPS. 1970. *Ap. J.* 162:105–12
Sackmann IJ, Weidemann V. 1972. *Ap. J.* 178:427–32
Salasnich B, Bressan A, Chiosi C. 1999. *Astron. Astrophys.* 342:131–52
Sandage AR. 1955. *Ap. J.* 122:263–70
Sandage AR, Schwarzschild M. 1952. *Ap. J.* 116:463–76
Sasselov DD. 1986. *Publ. Astron. Soc. Pac.* 98:561–71
Schaerer D, Contini T, Kunth D. 1999. *Astron. Astrophys.* 341:399– 417
Schaifers K, Voigt HH. 1982. *Astronomy and Astrophysics–stars and star clusters* Landolt–Bornstein New Series. Berlin: Springer Verlag 2b, 456 pp.
Schaller G, Schaerer D, Meynet G, Maeder A. 1992. *Astron. Astrophys. Suppl. Ser.* 96:269–331
Schatzman E. 1993. *Astron. Astrophys.* 279:431– 46
Schatzman E, Maeder A, Angrand F, Glowinsky R. 1981. *Astron. Astrophys.* 96:1–16
Schild H, Maeder A. 1984. *Astron. Astrophys.* 136:237– 42
Schmidt-Kaler Th. 1982. See Schaifers & Voigt, p. 1
Schönberner D, Herrero A, Becker S, Eber F, Butler K, et al. 1988. *Astron. Astrophys.* 197:209–22
Schulte-Ladbeck RE, Meade MR, Hillier DJ. 1992. See Drissen et al 1992, pp. 118–29
Schwarzschild M. 1958. In *Structure and Evolution of the Stars*, Princeton: Princeton Univ. Press, p. 183
Shindo M, Hashimoto M, Eriguchi Y, Müller E. 1997. *Astron. Astrophys.* 326:177–86
Slettebak A. 1966. *Ap. J.* 145:126–29
Slettebak A. 1970. In *Stellar Rotation*, IAU Coll. 4, ed. A Slettebak, pp. 3–8. Dordrecht: Reidel
Smith KC, Howarth ID. 1994. *Astron. Astrophys.* 290:868–74
Smith LF. 1973. In *W-R and High-Temperature Stars*, IAU Symp. 49, ed. MKV Bappu, J Sahade, pp. 15– 41. Dordrecht: Reidel
Smith LJ. 1988. *Ap. J.* 327:128–38
Smith LJ. 1997. See Nota & Lamers 1997, pp. 310–15
Smith LJ, Maeder A. 1998. *Astron. Astrophys.* 334:845–56
Sofia S, Howard JM, Demarque P. 1994. In *Pulsation; Rotation; and Mass Loss in Early-Type Stars*, IAU Symp. 162, ed. LA Balona, et al, pp. 131– 44. Dordrecht: Kluwer
Spiegel EA, Zahn JP. 1992. *Astron. Astrophys.* 265:106–114
Spruit HC, Knobloch E. 1984. *Astron. Astrophys.* 132:89–96
Spruit HC, Phinney ES. 1998. *Nature* 393:139–41
Sreenivasan SR, Wilson WJF. 1982. *Ap. J.* 254:287–96
Sreenivasan SR, Wilson WJF. 1985a. *Ap. J.* 290:653–59
Sreenivasan SR, Wilson WJF. 1985b. *Ap. J.* 292:506–10
Stothers RB. 1999. *Ap. J.* 513:460–63
Stothers RB, Chin CW. 1973. *Ap. J.* 179:555–68
Stothers RB, Chin CW. 1975. *Ap. J.* 198:407–17
Stothers RB, Chin CW. 1979. *Ap. J.* 233:267–79
Stothers RB, Chin CW. 1992a. *Ap. J.* 390:136–43
Stothers RB, Chin CW. 1992b. *Ap. J.* 390:L33–35
Stothers RB, Chin CW. 1993. *Ap. J.* 408:L85–88
Stothers RB, Chin CW. 1996. *Ap. J.* 468:842–50
Stothers RB, Chin CW. 1997. *Ap. J.* 489:319–30
Stothers RB, Chin CW. 1999. *Ap. J.* 522:960–64
Strittmatter PA. 1969. *Annu. Rev. Astron. Astrophys.* 7:665–84
Sweet PA. 1950. *MNRAS* 110:548–58
Takeda Y, Takada-Hidai M. 1995. *Publ. Astron. Soc. Jpn.* 47:169–88

Talon S, Zahn JP. 1997. *Astron. Astrophys.* 317:749–51

Talon S, Zahn JP. 1998. *Astron. Astrophys.* 329:315–18

Talon S, Zahn JP, Maeder A, Meynet G. 1997. *Astron. Astrophys.* 322:209–17

Tassoul JL. 1978. In *Theory of Rotating Stars*, Princeton: Princeton Univ. Press

Tassoul JL. 1990. In *Angular Momentum and Mass Loss for Hot Stars*, ed. LA Willson, R Stalio, pp. 7–32. Dordrecht: Kluwer

Tassoul JL, Tassoul M. 1982. *Ap. J. Suppl.* 49:317–50

Tassoul JL, Tassoul M. 1995. *Ap. J.* 440:789–809

Thé PS, Arens M, van der Hucht KA. 1982. *Astrophys. Lett.* 22:109–18

Thuan TX, Izotov YJ, Lipovetsky VA. 1995. *Ap. J.* 445:108–23

Toomre L. 1994. *AAS* 184.5002

Trimble V, Rees MJ. 1970. *Astrophys. Lett.* 5: 93

Tutukov AV, Yungelson LR. 1985. *Sov. Astron.* 29:352

Ulmer A, Fitzpatrick EL. 1998. *Ap. J.* 504:200–6

Urpin VA, Shalybkov DA, Spruit HC. 1996. *Astron. Astrophys.* 306:455– 463

van der Hucht KA. 1992. *Astron. Astrophys. Rev.* 4:123–59

van der Hucht KA. 1999. See van der Hucht et al 1999, pp. 13–20

van der Hucht KA, Koenigsberger G, Eenens PRJ. 1999. *Wolf-Rayet Phenomena in Massive Stars and Starburst Galaxies*, IAU Symp. 193. San Francisco: Astron. Soc. Pacific, 788 pp.

Vauclair, S. 1999. *Astron. Astrophys.* 351:973–80

Vardya MS. 1985. *Ap. J.* 299:255–64

Venn KA. 1995a. *Ap. J.* 449:839–62

Venn KA. 1995b. *Ap. J. Suppl.* 99:659–92

Venn KA. 1998. See Howarth 1998, pp. 177–87

Venn KA. 1999. *Ap. J.* 518:405–21

Venn KA, Lambert DL, Lemke M. 1996. *Astron. Astrophys.* 307:849–59

Verdugo E, Talavera A, Gómez de Castro AI. 1999. *Astron. Astrophys.* 346:819–30

Villamariz MR, Herrero A. 2000. *Astron. Astrophys.* In press.

Viotti R, Rossi L, Cassatella A, Altmore A, Baratta GB. 1989. *Ap. J. Suppl.* 71:983–1009

Voels SA, Bohannan B, Abbott DC, Hummer DG. 1989. *Ap. J.* 340:1073–190

Vogt H. 1925. *Astron. Nachr.* 223:229

von Zeipel H. 1924. *MNRAS* 84:665–701

Walborn NR. 1988. In *Atmospheric Diagnostics of Stellar Evolution*, IAU Coll. 108, ed. K Nomoto, pp. 70–78. New York: Springer

Waters LBFM. 1997. See Nota & Lamers 1997, pp. 326–31

Weiss A. 1994. *Astron. Astrophys.* 284:138– 44

Weiss A, Hillebrandt W, Truran JW. 1988. *Astron. Astrophys.* 197:L11–14

Willis AJ. 1991. See Michaud & Tutukov 1991, pp. 195–207

Willis AJ. 1999. See van der Hucht et al 1999, pp. 1–12

Willis AJ, Dessart L, Crowther PA, Morris PW, Maeder A, Conti PS, van der Hucht KA. 1997. *MNRAS* 290:371–79

Willis AJ, Dessart L, Crowther PA, Morris PW, van der Hucht KA. 1998. *Astrophys. and Space Sc.* 255:167–8

Wolf G, Stahl O, Fullerton AW. 1999. *Variable and Non-Spherical Winds in Luminous Hot Stars*, IAU Coll. 169, Lecture Notes in Physics 523. Heidelberg: Springer Verlag 424 pp.

Woosley SE. 1986. In *Nucleosynthesis and Chemical Evolution*, 16th Saas-Fee Course, ed. A Maeder, B Hauck, G Meynet, pp. 1–195. Geneva: Geneva Observatory

Woosley SE. 1993. *Ap. J.* 405:273–77

Woosley SE, Heger A, Weaver TA, Langer N. 2000. In *SN 1987A: Ten Years After*, ed. MM Phillips, NB Suntzeff, Fifth CTIO/ESO/LCO Workshop. In press

Zahn JP. 1974. In *Stellar Instability and Evolution*, IAU Symp. 59, ed. P Ledoux, et al, pp. 185–195. Dordrecht: Reidel

Zahn JP. 1983. In *Astrophysical Processes in*

Upper Main Sequence Stars, ed. B Hauck, A Maeder, Saas Fee Course, pp. 253–329. Geneva: Geneva Observatory

Zahn JP. 1992. *Astron. Astrophys.* 265:115–32

Zahn JP. 1994. *Space Sci. Rev.* 66:285–97

Zahn JP, Talon S, Matias J. 1997. *Astron. Astrophys.* 332:320–28

Zickgraf FJ. 1999. See Wolf et al 1999, pp. 40–48

Annual Review of Astronomy and Astrophysics
Volume 38, 2000

CONTENTS